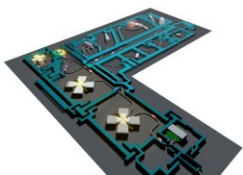


# Nuclear Physics Highlights from Stable Ion Beam Facilities ECOS -2011-2014

*A. Navin*

*Grand Accélérateur National d'Ions Lourds, France*



Julin Rauno



Fanny, Maurice, Christelle, John +

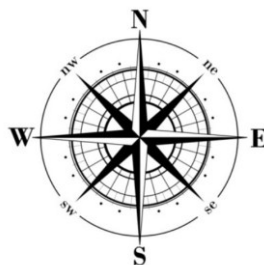
Georgi Iulian, Iolanda+



ŚRODOWISKOWE LABORATORIUM  
CIĘŻKICH JONÓW



Pawel  
Krzyszto



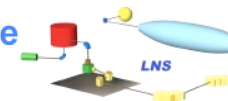
Adam

Giacomo, Lorenzo

Laboratori Nazionali di Legnaro



Istituto Nazionale di Fisica Nucleare  
Laboratori Nazionali del Sud



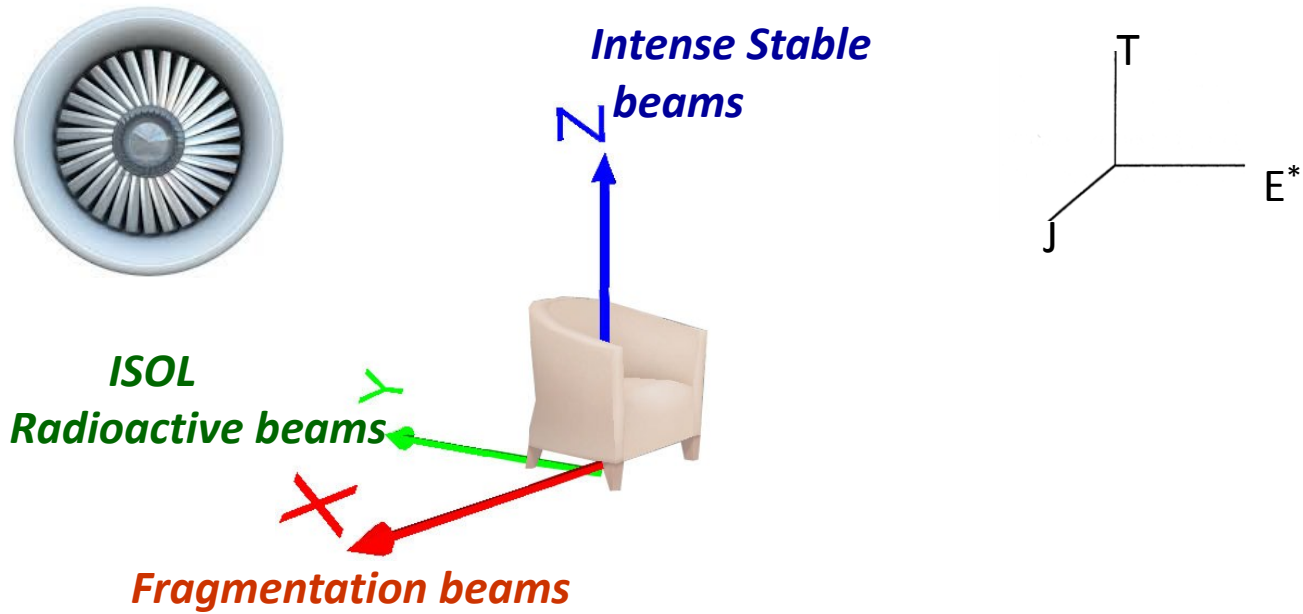
Stefano Romano +

- ALTO-IPN - Orsay/France
- GANIL - Caen/France
- GSI - Darmstadt/Germany
- IFJ - Cracow/Poland
- JYFL - Jyväskylä/Finland
- LNL-INFN - Legnaro/Italy
- LNS-INFN - Catania/Italy
- SLCJ - Warsaw/Poland

Inputs from the various labs  
Work from many institutions



# Plan of the talk



A variety of Physics Q's (suggested by the labs)

Tools and phenomena      Selectivity and sensitivity

Tomorrow ?

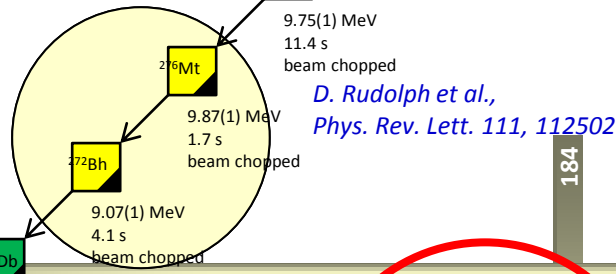
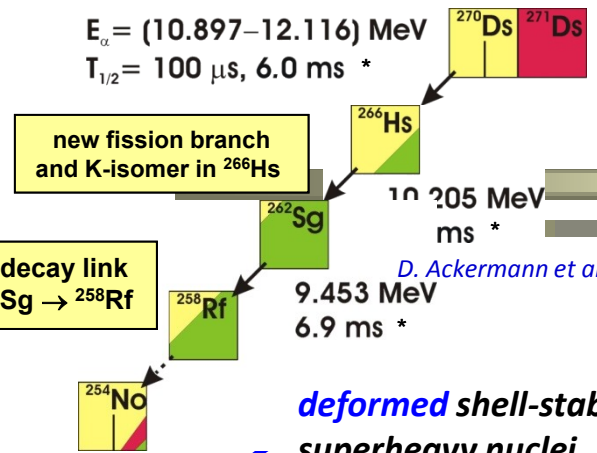
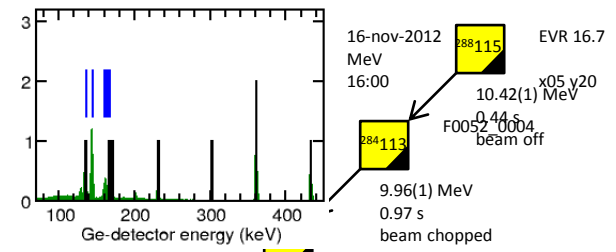
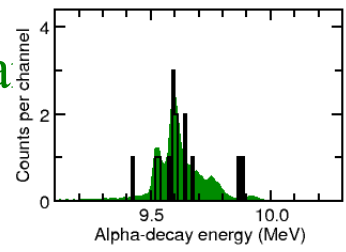
# SHE resea

## SHE Synthesis

- hot fusion: confirmation at LBNL and GSI for Z=112, 114, 115, 116, 117
- first attempt to fix Z via X-ray detection for <sup>288</sup>115

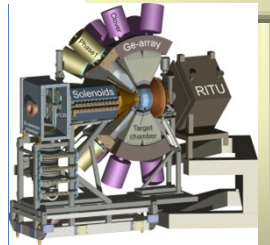
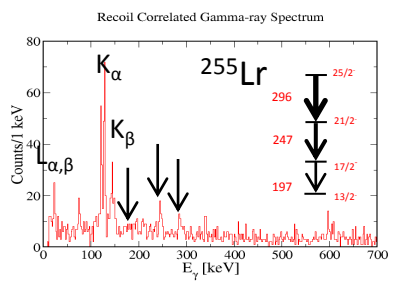
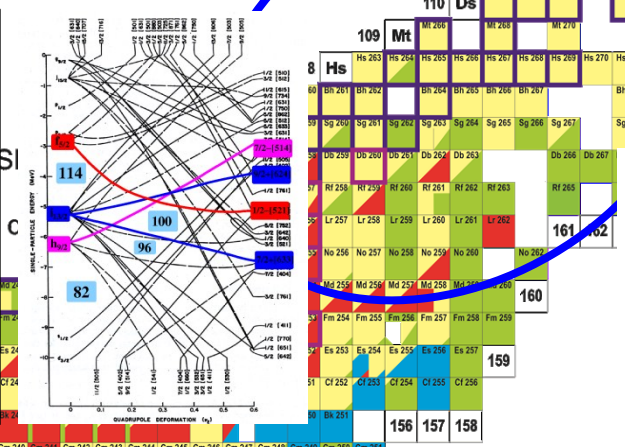
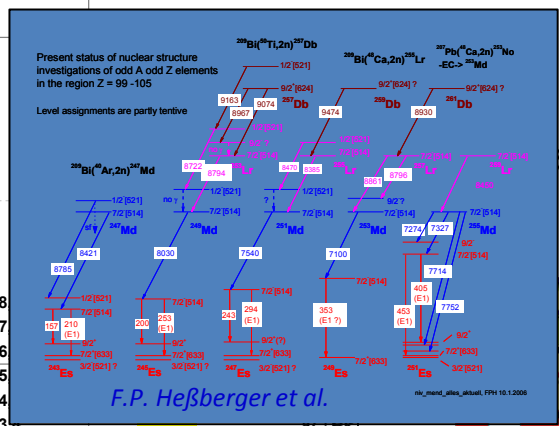
## nuclear structure features of superheavy nuclei

- new approaches
- precise masses for nobelium and lawrencium from SHIPTRAP
- E<sub>bind</sub>
- laser spectroscopy beyond fermium

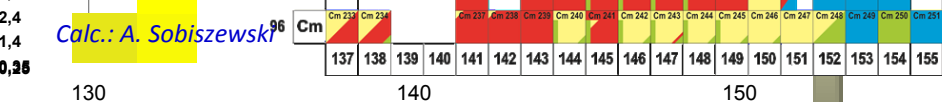


**spherical shell-stabilised superheavy nuclei**

**deformed shell-stabilised superheavy nuclei**

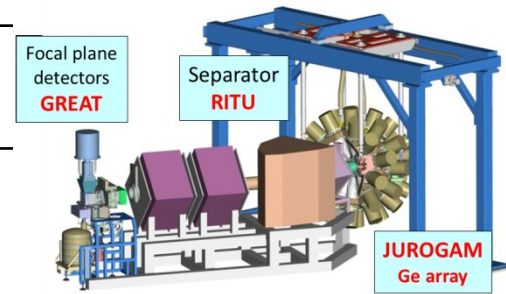


M. Sandzelius et al., Zakopane 2014



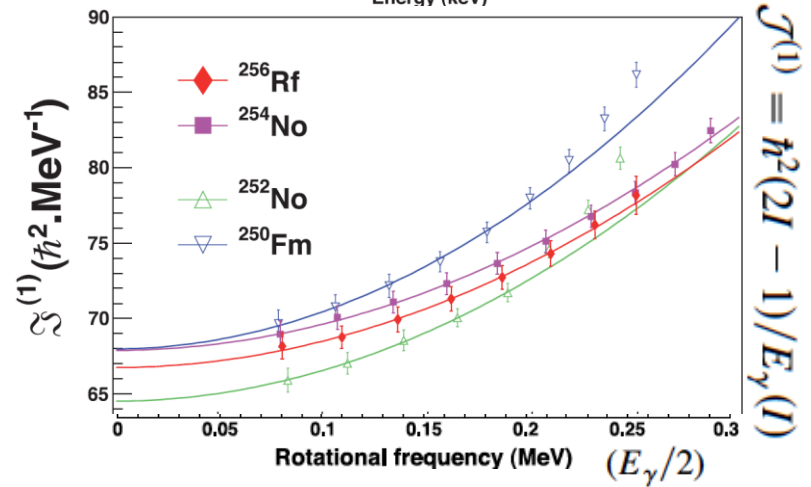
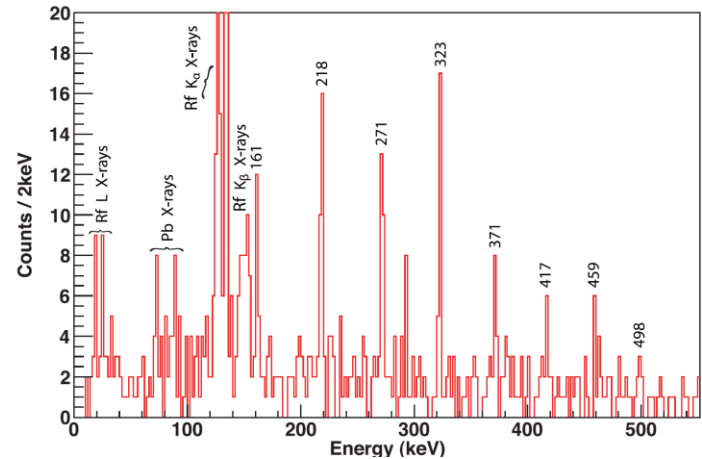
# Shell-structure and pairing interaction in superheavy nuclei: Rotational properties of the $Z=104$ nucleus $^{256}\text{Rf}$

## JYFL - Jyväskylä



### At the high-Z limit of in-beam spectroscopy:

- ❑  $^{208}\text{Pb}(^{50}\text{Ti}, 2n)^{256}\text{Rf}$  - 17nbarn
- ❑ Gammapool detectors + RITU-GREAT
- ❑ High rates with digital electronics
- ❑ Strasbourg contribution in beam development



At a deformed shell gap, the pairing correlations are weakened, which in turn leads to a larger moment of inertia. This seems to be borne out by the behavior of the moments of inertia  $I$  available. It might also be expected that if there is a significant shell gap at  $Z = 104$ , that the moment of inertia of  $^{256}\text{Rf}$  would be larger than that of the isotope  $^{254}\text{No}$ .

$J(1) \rightarrow$  no  $Z = 104$  shell gap

Selected for a Viewpoint in *Physics*  
PHYSICAL REVIEW LETTERS

week ending  
6 JULY 2012

Shell-Structure and Pairing Interaction in Superheavy Nuclei:  
Rotational Properties of the  $Z=104$  Nucleus  $^{256}\text{Rf}$

# JYFL – Jyväskylä: MARA ready soon

A new vacuum-mode separator – MARA  
→ better mass selection in RDT experiments

Focal plane  
+ gas cell

MD

ED

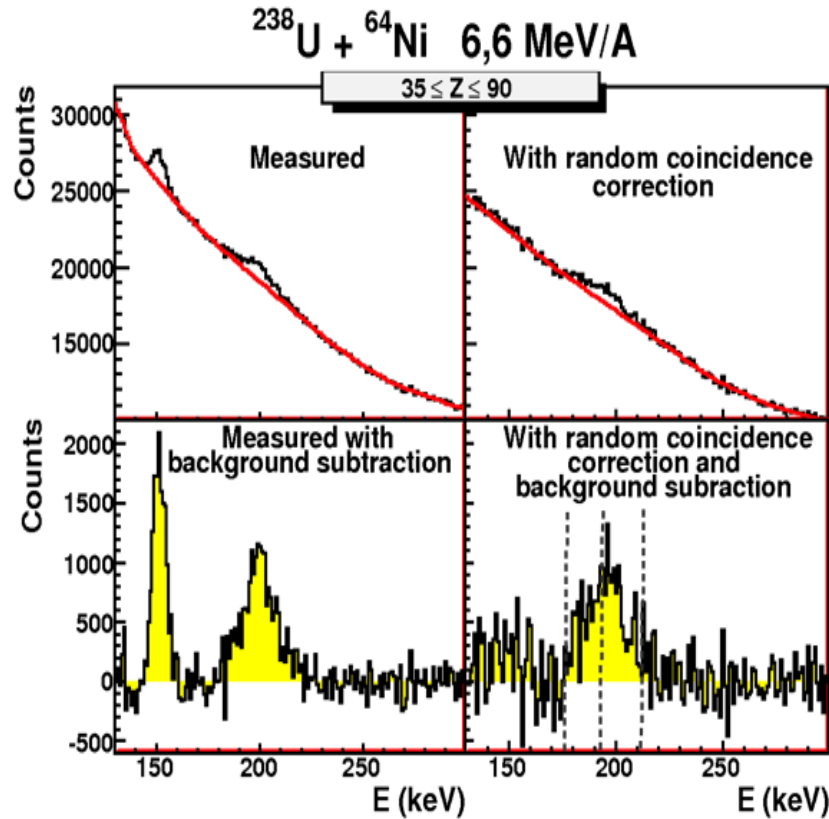
QQQ

Beam

- Solid angle acceptance (central  $m/q$  and energy) 10 msr
- Typical transmission  $\sim 12\%$  per charge state



# Fission life-times : a link towards the production of SHE

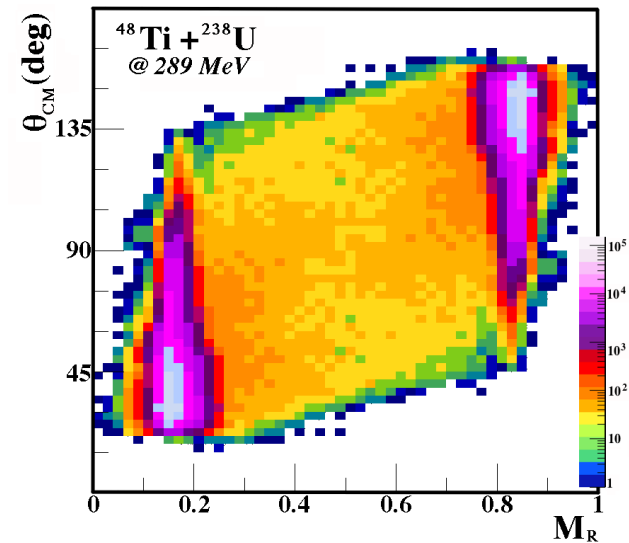


New Collaboration:

**GANIL-IPNO-SPhN?-ANU**

*Measure in coincidence with X-rays*

*The angular distribution of fragments*



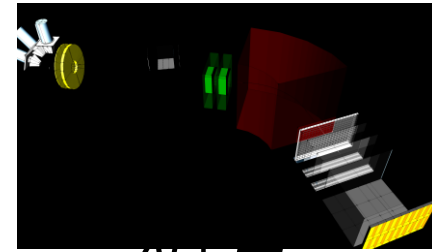
*M.O. Frégeau et al., Phys. Rev. Lett. 108, 12270 (2012)*

- $X_K$  fluorescence of the atom with 120 protons has been observed.
- Compound nucleus lifetime of the order of the K-vacancy lifetime ( $\sim 10^{-18}\text{s}$ )

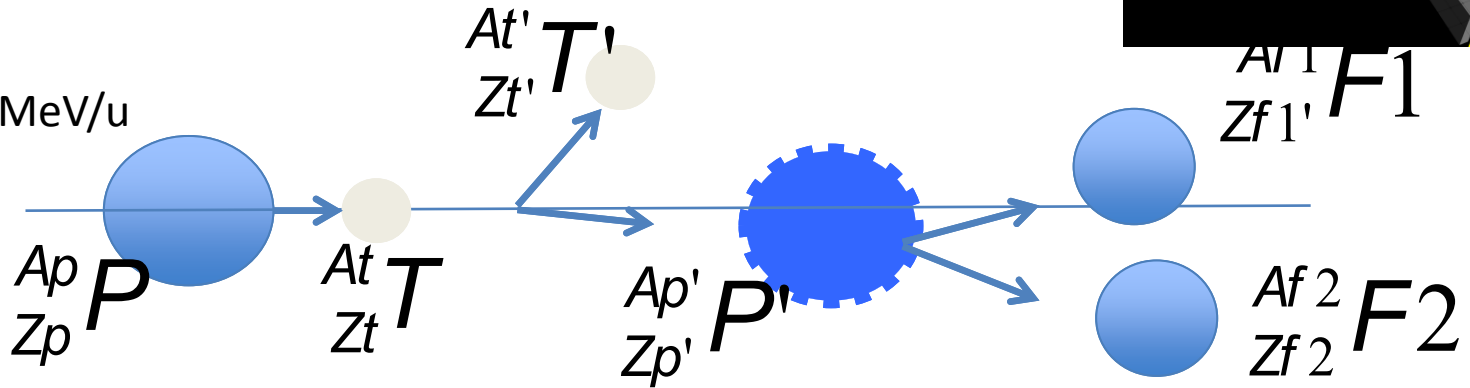
- Determination of the fusion components on  $4\pi$  from X-ray fluorescence
- Reconcile the most probable fission times inferred from angular distributions with the average fission times inferred from direct measurements

# Transfer-induced fission in inverse kinematics @ GANIL

F. Farget et al., GANIL

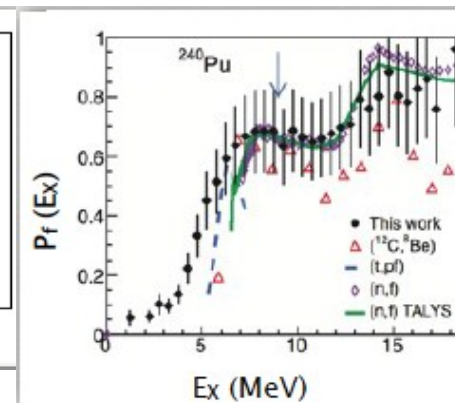
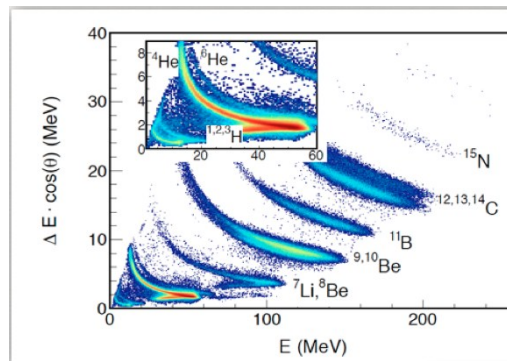


$^{238}\text{U} + ^{12}\text{C}$  @ 6.1 MeV/u



242 Cf	243 Cf	244 Cf	245 Cf	246 Cf	247 Cf	248 Cf	249 Cf	250 Cf	251 Cf	252 Cf
241 Bk	242 Bk	243 Bk	244 Bk	245 Bk	246 Bk	247 Bk	248 Bk	249 Bk	250 Bk	251 Bk
240 Cm	241 Cm	242 Cm	243 Cm	244 Cm	245 Cm	246 Cm	247 Cm	248 Cm	249 Cm	250 Cm
239 Am	240 Am	241 Am	242 Am	243 Am	244 Am	245 Am	246 Am	247 Am	248 Am	249 Am
238 Pu	239 Pu	240 Pu	241 Pu	242 Pu	243 Pu	244 Pu	245 Pu	246 Pu	247 Pu	
237 Np	238 Np	239 Np	240 Np	241 Np	242 Np	243 Np	244 Np			
236 U	237 U	238 U	239 U	240 U	241 U	242 U				

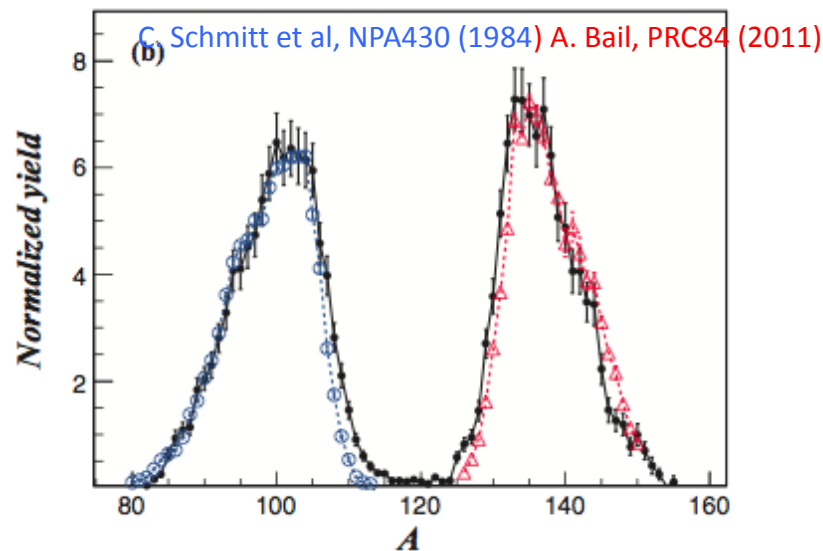
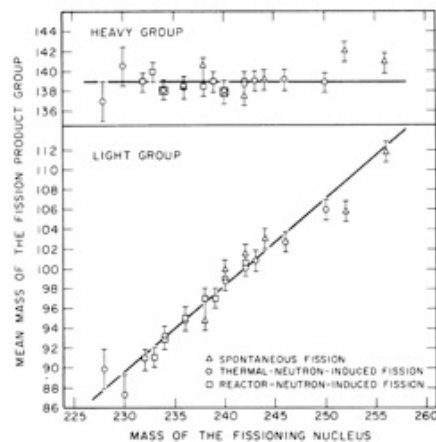
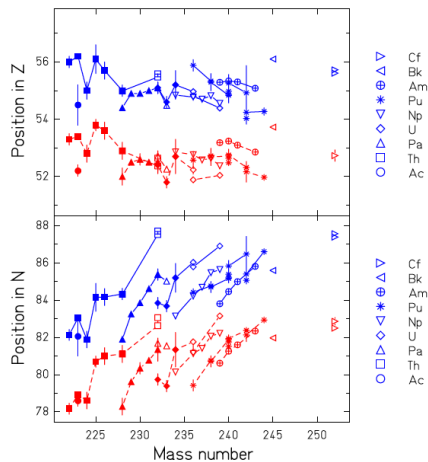
- 10 actinides produced
- $E^*$  distribution
- Full resolution in (Z,A) of fragments
- TKE



*Applications reactor heat, radio toxicity control*

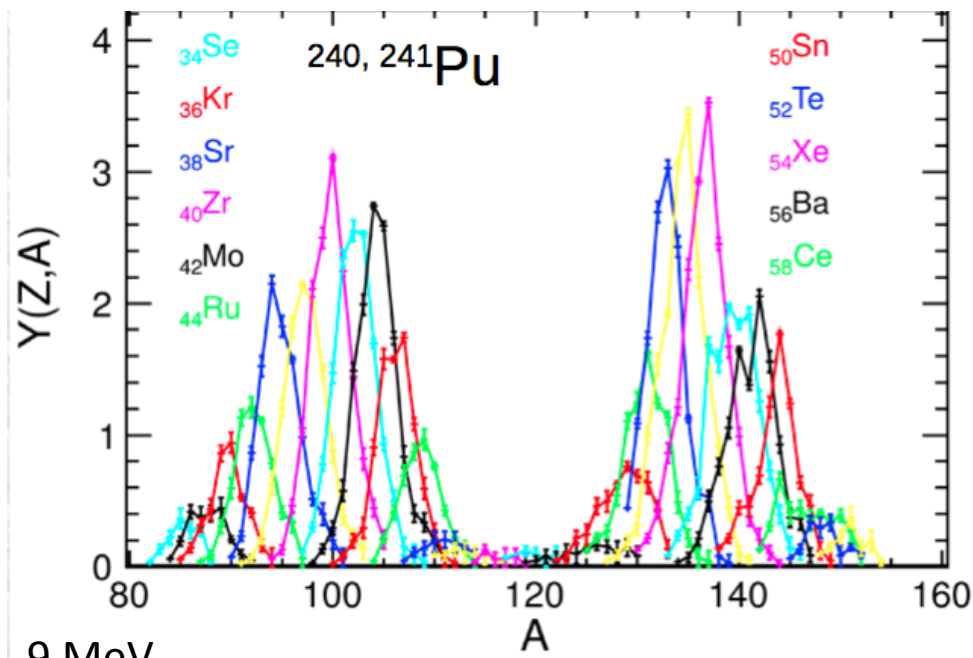
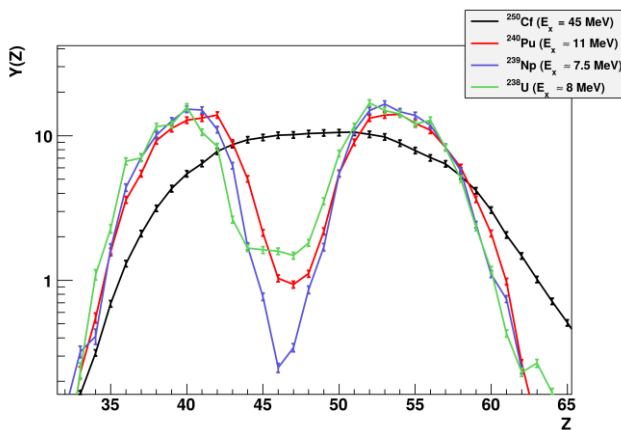
# Isotopic distribution of fission fragments : Open Questions

F. Farget et al., GANIL



Z=54: N=82;86-90

M. Caamaño et al., PRC 88 (2013) 024605

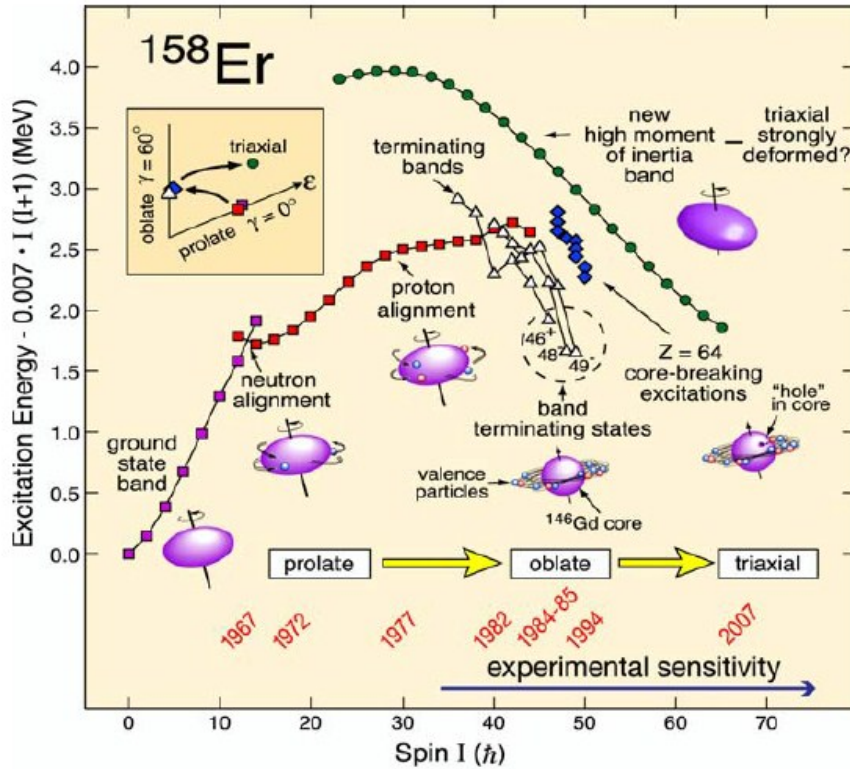
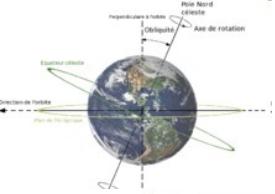


8 MeV

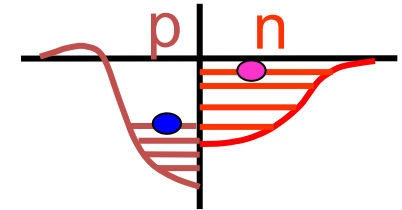
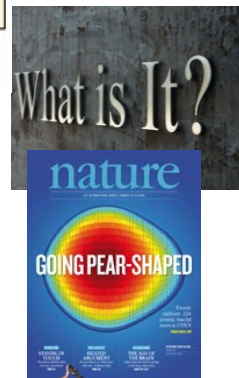
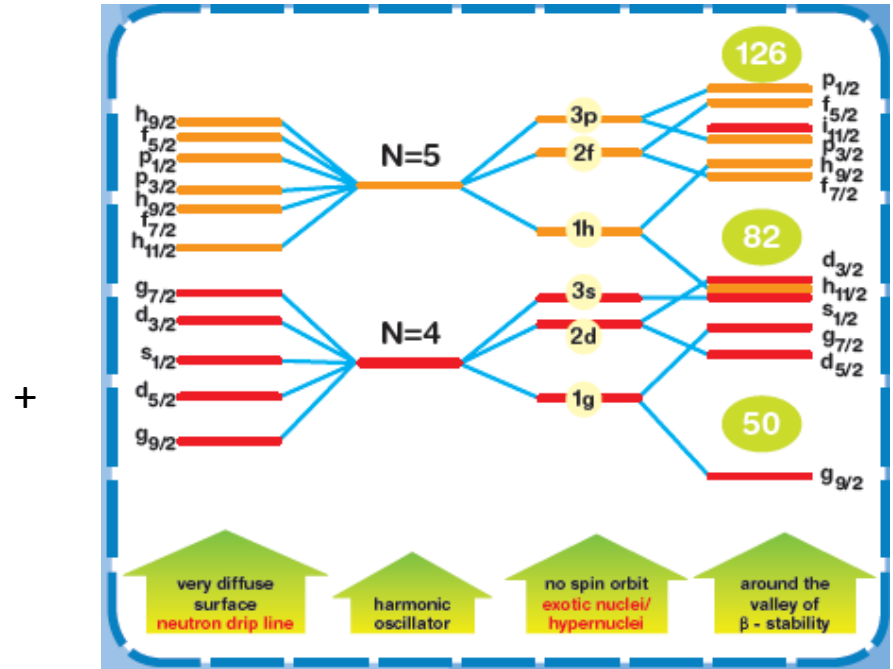
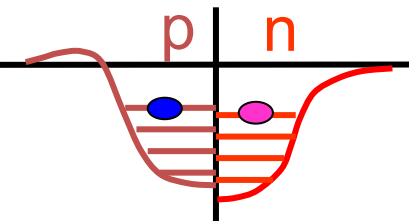


# What happens when an exotic nuclei undergoes fast rotation

Is this the next question we want to address

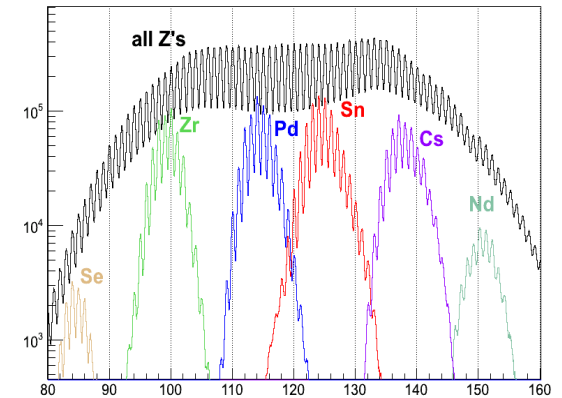
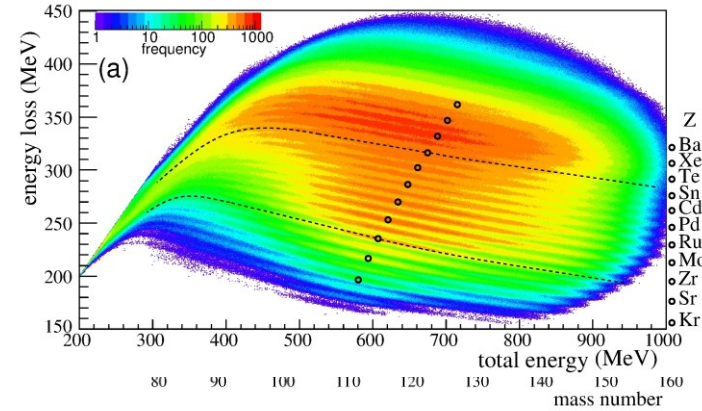
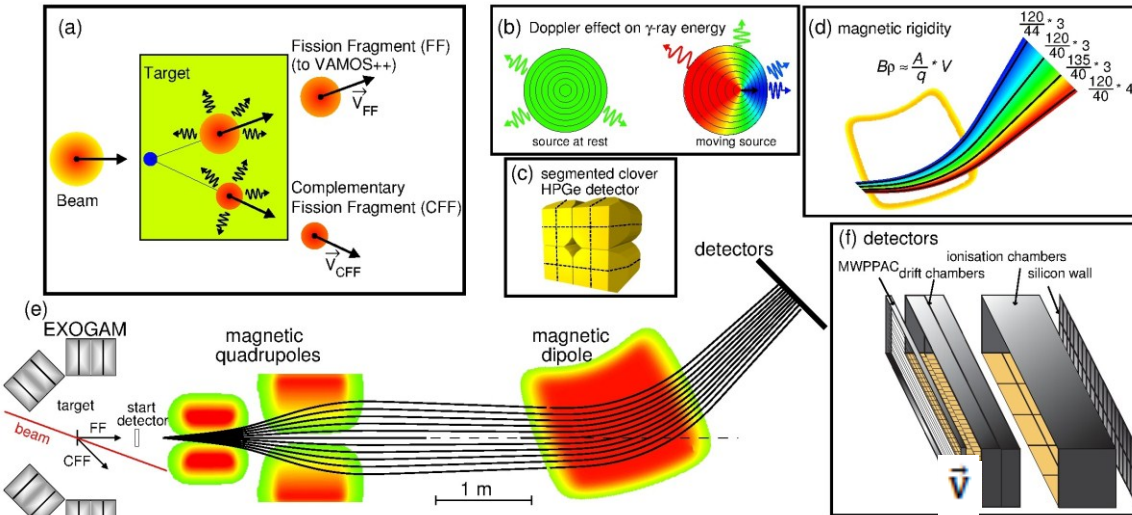


AIP Conf. Proc. 1498, 84 (2012)



Look for new "effects"  
With the next level of sensitivity

# Prompt spectroscopy of $M$ and $Z$ identified fission frag



*Thus uniquely identify  $M$  and  $Z$   
 Doppler correction for the emitted  $\gamma$  rays  
 $\vec{V}$  of the fragment & angle of the segment of the clover detector*

$^{238}\text{U} + ^9\text{Be}$  at 6 MeV/U

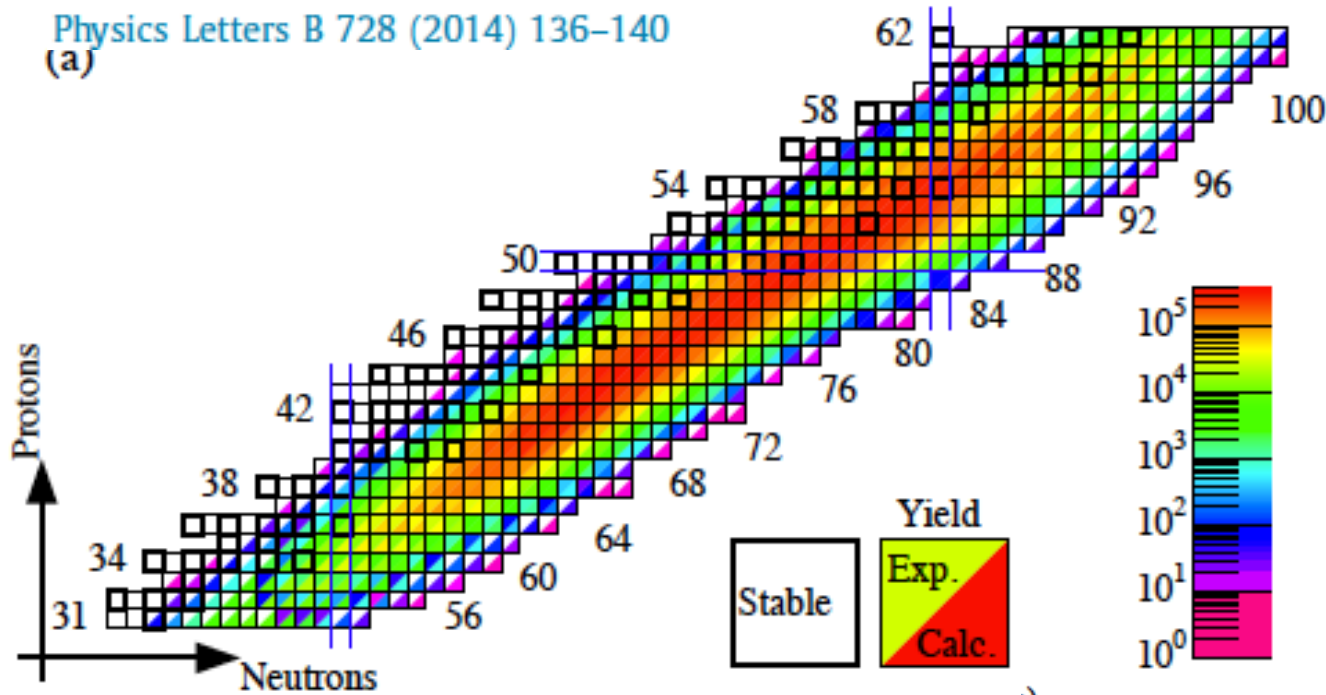
Tomorrow AGATA@GANIL

# Fission fragment spectroscopy

Towards The next frontier of Nuclear Physics: High Spin *and* Isospin

Physics Letters B 728 (2014) 136–140

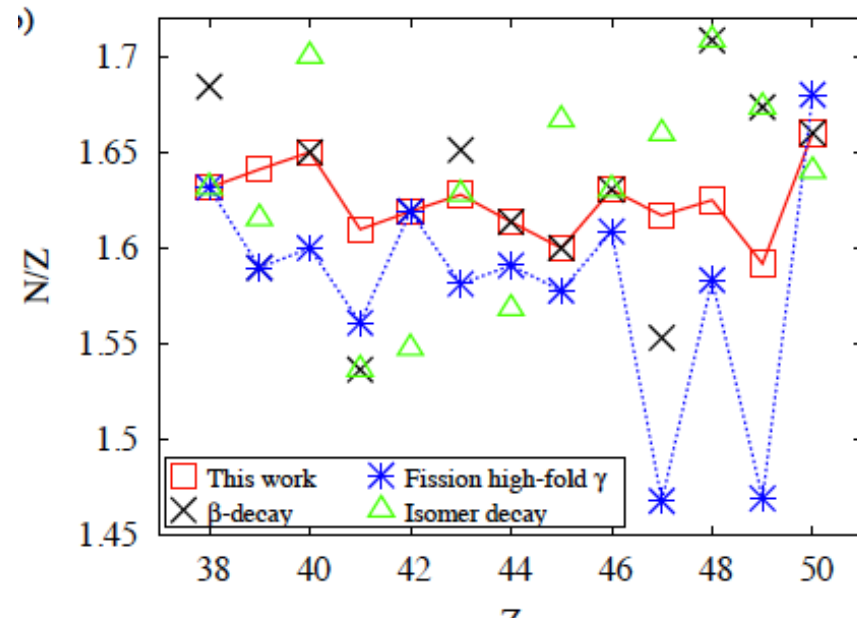
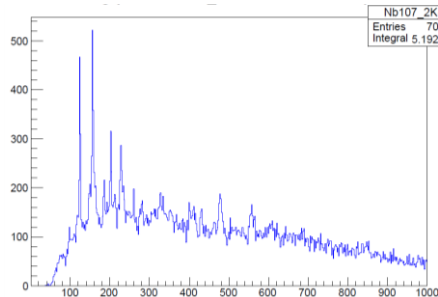
(a)



Limit of Mass distb<sup>n</sup> from  
The Fission mechanism  
Not acceptance

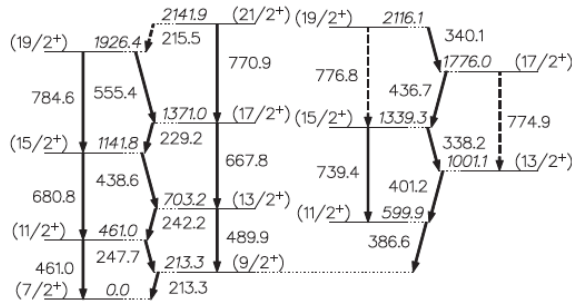
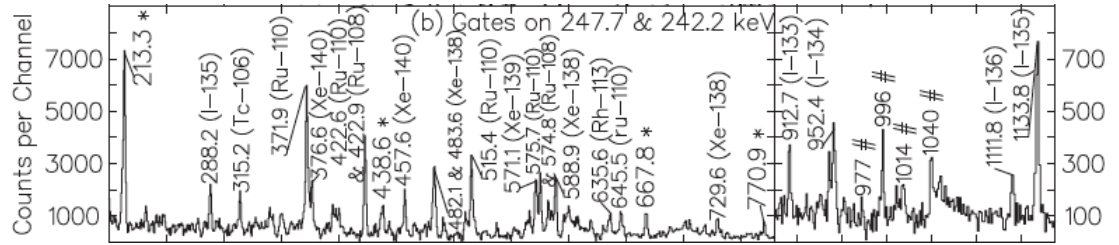
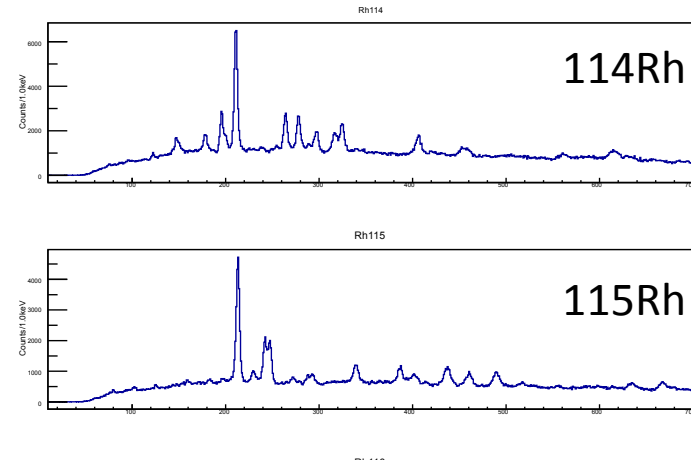
Measurements of Yields and Gamma rays

FF yields as low as  $\sim 2.5 \cdot 10^{-5}$  measured ( $^{106}\text{Zr}$ )



II)

# Neutron Rich $_{45}\text{Rh}$



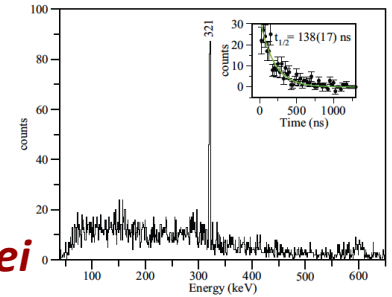
$\gamma$ - spectroscopy till  $^{115}\text{Rh}$  (Cf  $\gamma$ -Sphere  $\gamma$ - $\gamma$ - $\gamma$ - $\gamma$ )  
S.H. Liu et al., PRC 84 014304 (2011)

Isomer 138ns  $^{117}\text{Rh}$  (GSI)  
S. Lakovski et al. PRC 88 024302 (2013)

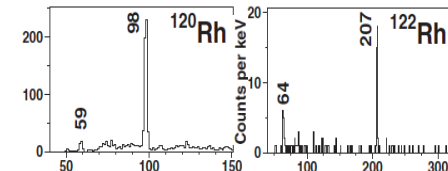
0.29, 0.82  $\mu\text{s}$   $^{120,122}\text{Rh}$   
D. Kameda et al., Phys. Rev. C 86, 054319 (2012)

FIG. 1. A high-spin level scheme of  $^{115}\text{Rh}$  built in the present

**regular and simple patterns  
that emerge  
in the structure of complex nuclei**



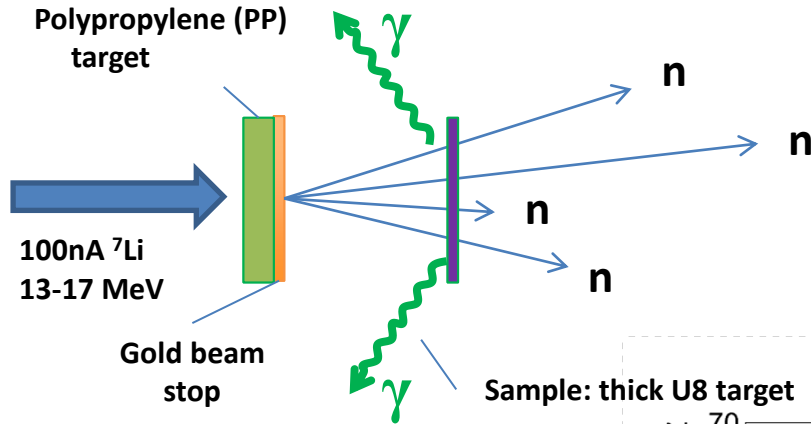
Work in progress





# Lithium Inverse Cinematiques ORsay Neutron source

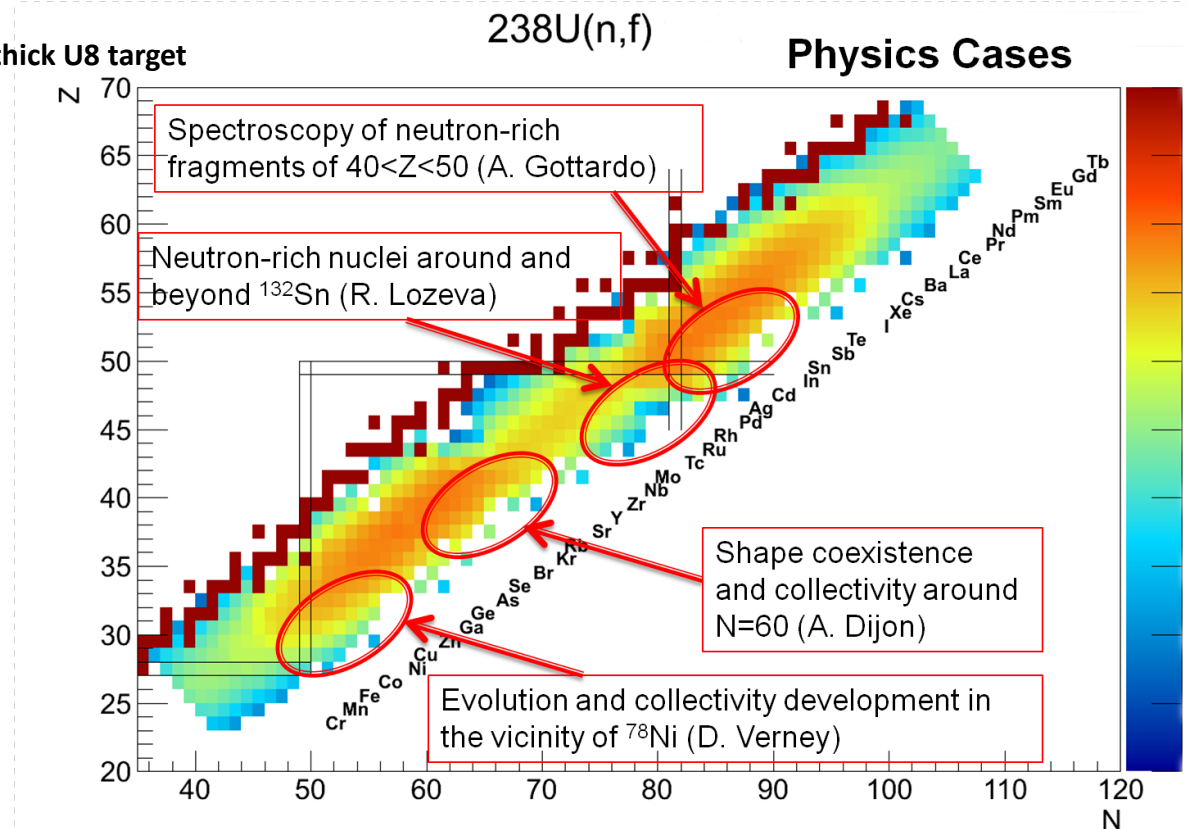
LICORNE



Intense focused monoenergetic neutron source:  
 **$10^7$  n/s/steradian**

## First LICORNE – ORGAM coupling: January 2014

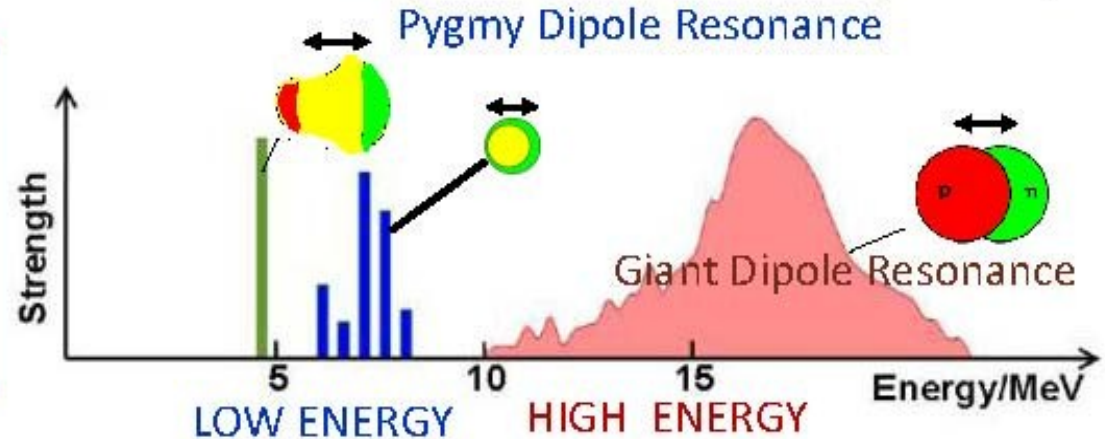
- Isomer tagging of fission partners
- H2 to replace PP target
- following experiment at IPN :  
ORGAM and Miniball (MINORCA)



# Isoscalar Component of the PDR for Nuclei with n-excess

Nuclear Structure information from the Low Energy part of the Electric Dipole response

The relevant energy window for  $(\gamma, n)$  reactions in the stellar photon bath is located in the vicinity of the PDR.



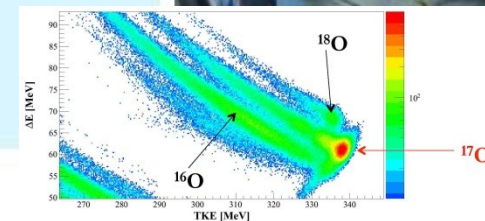
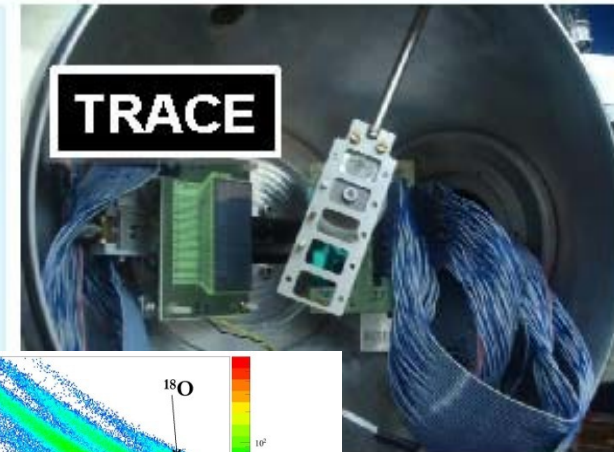
Inelastic scattering of  $^{17}\text{O}$  @ 20 MeV/u on different targets +  $\gamma$ -rays in coincidence

**HECTOR+**



## TWO EXPERIMENTS PERFORMED:

- ❑ Studied Nuclei:  **$^{208}\text{Pb}$   $^{90}\text{Zr}$**   
R. Nicolini (Università di Milano /INFN)  
D. Mengoni (Università di Padova /INFN)
- ❑ Studied nuclei:  **$^{208}\text{Pb}$ ,  $^{124}\text{Sn}$ ,  $^{140}\text{Ce}$**   
M. Kmiecik (IFJ PAN Kraków),  
F. Crespi (Univ. di Milano /INFN)

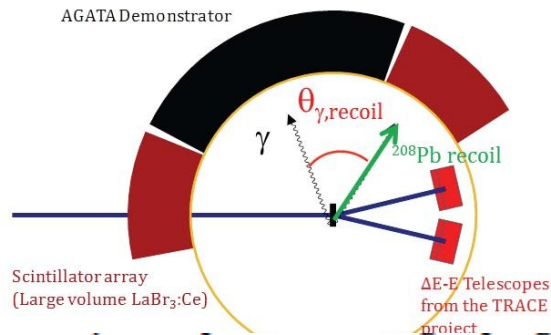
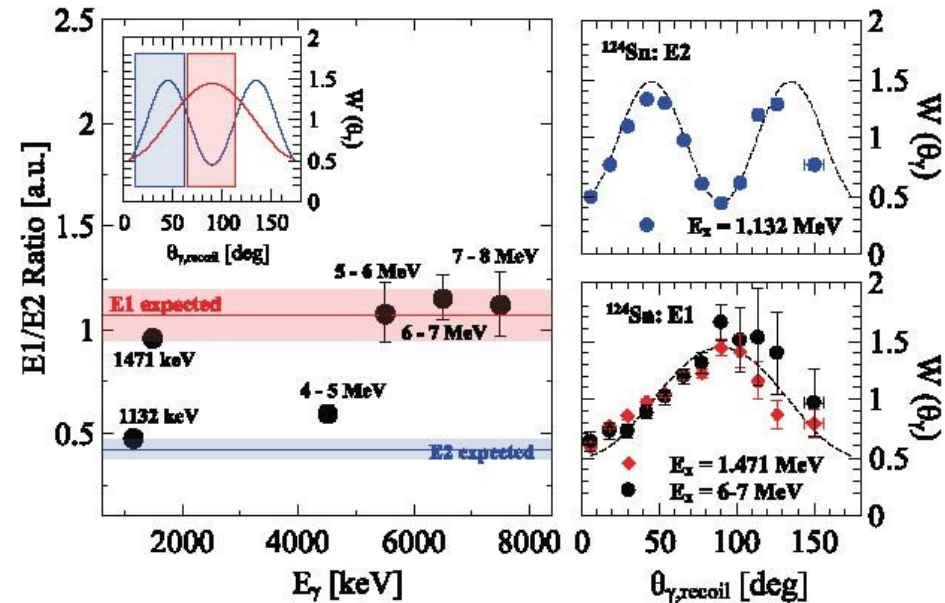
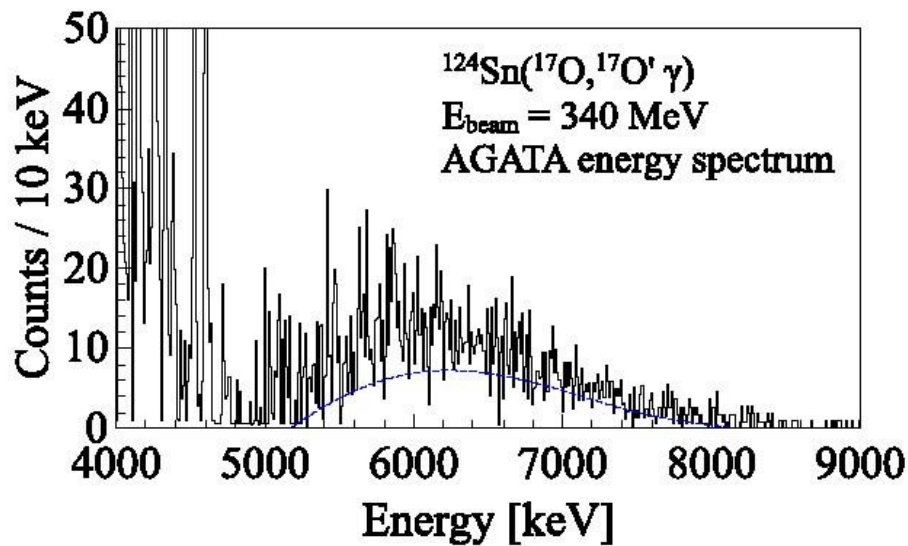


# Pygmy Dipole Resonance in $^{124}\text{Sn}$ by inelastic scattering of $^{17}\text{O}$

L. Pellegri Phys. Lett. B (in press)

Dominant Isoscalar excitation: n and p transition densities are **in phase** inside the nucleus, at the surface only the n-part survives

Inelastic scattering: Interaction Surface Peaked ( $^{17}\text{O}$ )

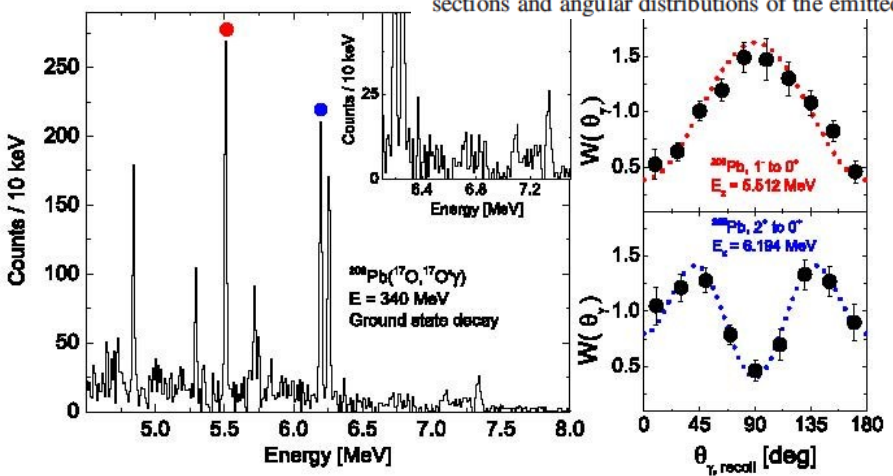


The emitted  $\gamma$  rays were detected with high resolution with the AGATA demonstrator array and the scattered ions were detected in two segmented  $\Delta E-E$  silicon telescopes.

# Isospin character of low-lying pygmy states in $^{208}\text{Pb}$ via inelastic scattering of $^{17}\text{O}$

F.C.L. Crespi et al., PRL 113, 012501 (2014)

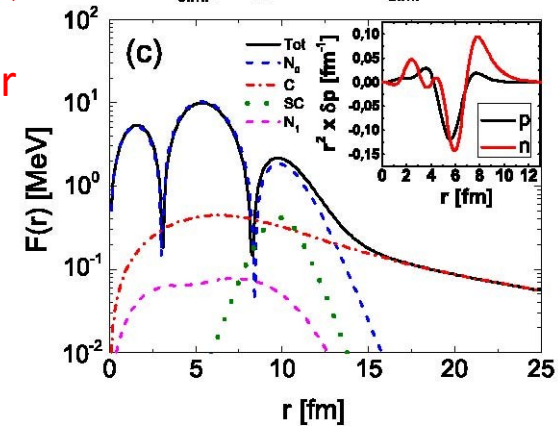
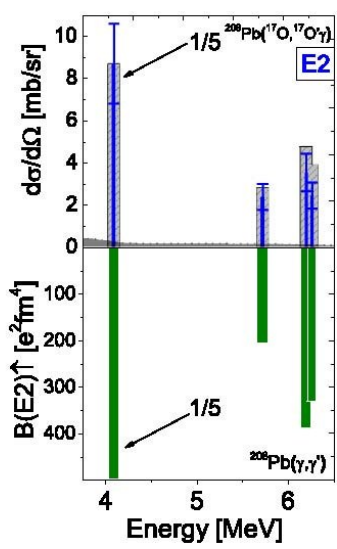
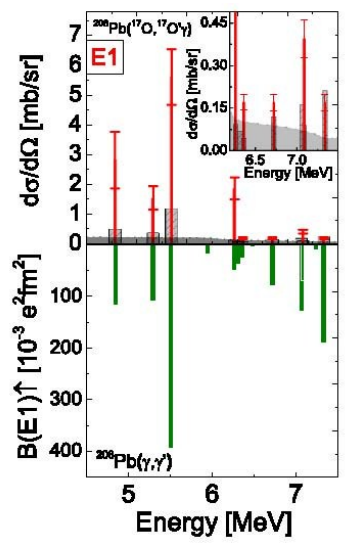
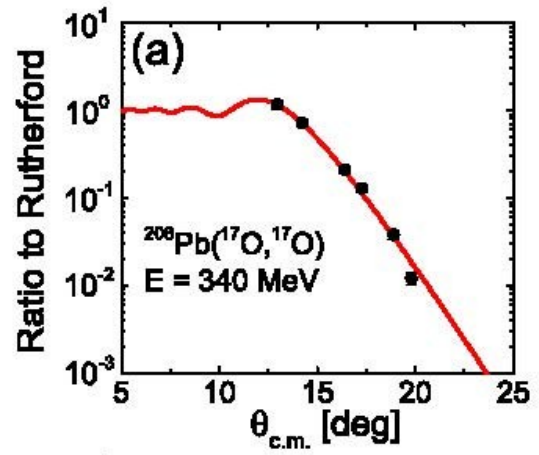
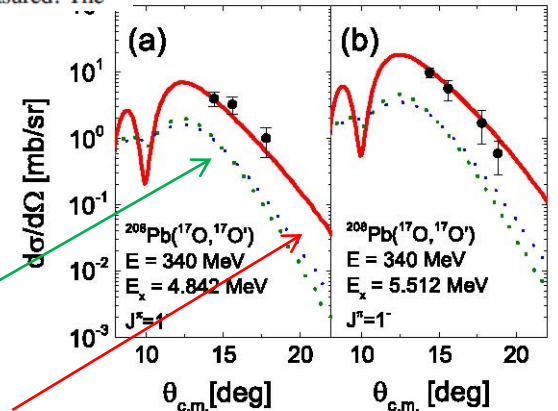
The properties of pygmy dipole states in  $^{208}\text{Pb}$  were investigated using the  $^{208}\text{Pb}(^{17}\text{O}, ^{17}\text{O}^*)\gamma$  reaction at 340 MeV and measuring the  $\gamma$  decay with high resolution with the AGATA demonstrator array. Cross sections and angular distributions of the emitted  $\gamma$  rays and of the scattered particles were measured. The



$^{208}\text{Pb}(^{17}\text{O}, ^{17}\text{O}^*)^{208}\text{Pb}^*$   
 E1 at 4.85 MeV and  
 5.54 MeV

Phenomenological  
 form factor, isovector

nuclear contribution  
 microscopic form factor



Nuclei with n-excess  
 show low-lying dipole  
 strength with strong  
 isoscalar component



# Isospin Character of Low-Lying Pygmy Dipole States in $^{208}\text{Pb}$ via Inelastic Scattering of $^{17}\text{O}$ Ions

The  $E1$  transitions cross sections for  $^{208}\text{Pb}$  were analyzed for the first time using a microscopic form factor and the isoscalar potential was found to depend on the presence of the neutron skin. A

Doctopic: Experiments

ARTICLE IN PRESS

PLB:30434

Physics Letters B ●● (●●●●) ●●-●●



ELSEVIER

Contents lists available at [ScienceDirect](http://ScienceDirect)

Physics Letters B

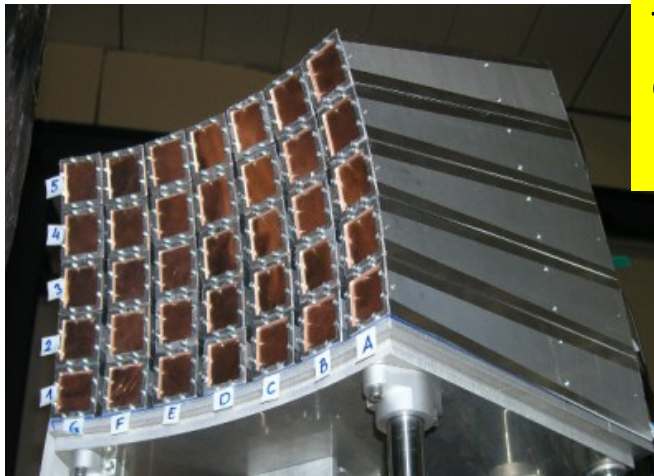
[www.elsevier.com/locate/physletb](http://www.elsevier.com/locate/physletb)

Pygmy dipole resonance in  $^{124}\text{Sn}$  populated by inelastic scattering of  $^{17}\text{O}$

For the  $1^-$  states a DWBA analysis based on a microscopically calculated form factor was performed and showed a sensitivity to the surface part of the transition density. Being the transition density dominated on the surface by the neutron component one can deduce that the pygmy states  $^{124}\text{Sn}$  are associated with the excitation of surface neutrons, mainly those in the neutron skin. Therefore in the future it will be very interesting to perform these studies on the isotopic chain of Sn and other neutron-rich nuclei also using other probes as protons at medium energy.

## A) Study of collective modes excited by high-energy protons

1. **HECTOR** array to measure high energy gamma-rays



2. **KRATTA** array (triple CsI telescopes) at forward direction to measure the energy of inelastically scatter protons

3\*. **PARIS Demonstrator** for PDR measurements with high-resolution, in coincidence with KRATTA



\* - in dedicated campaigns



# Hot GDR study in nuclei in the mass region $A \sim 120-132$ with MEDEA at LNS

Onset of the quenching of the Giant Dipole Resonances at high excitation energies

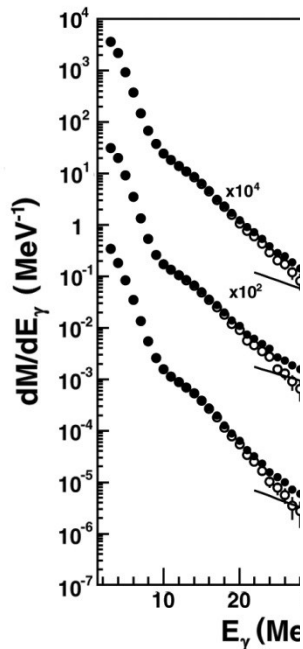
D.Santonocito<sup>a)</sup>, Y.Blumenfeld<sup>b)</sup>, C. Agodi<sup>a)</sup>, R.Alba<sup>a)</sup>, G. Bellia<sup>a),c)</sup>, R. Coniglione<sup>a)</sup>,  
 F. Delaunay<sup>b)\*</sup>, A. Del Zoppo<sup>a)</sup>, P. Finocchiaro<sup>a)</sup>, F. Hongmei<sup>a)</sup>, V. Lima<sup>b)</sup>, C.  
 Maiolino<sup>a)</sup>, E. Migneco<sup>a),c)</sup>, P.Piattelli<sup>a)</sup>, P. Sapienza<sup>a)</sup>, J.A. Scarpaci<sup>b)†</sup>, O.Wieland<sup>d)</sup>

*The evolution of the Giant Dipole Resonance properties in nuclei of mass  $A = 120-132$  has been investigated in an excitation energy range between 150 and 270 MeV through the study of complete and nearly complete fusion reactions. Evidence of a quenching of the GDR gamma yield was found at 270 MeV excitation energy.*

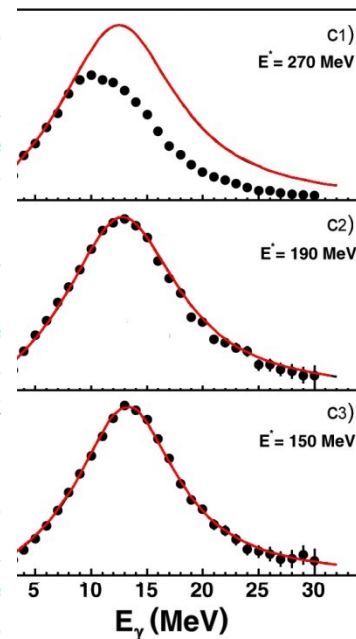
*A limiting excitation energy for the collective motion of about  $E^*/A \sim 2$  MeV/A was extracted.*

$^{116}\text{Sn}+^{12}\text{C}$  17A MeV  
 $^{116}\text{Sn}+^{12}\text{C}$  23A MeV  
 $^{116}\text{Sn}+^{24}\text{Mg}$  17A MeV

$E^*$	$A_{\text{res}}$
150	124
190	123
270	132



for mass  $A \sim 132$ . Evidence of a limiting excitation for the collective motion was also extracted in nuclei of mass  $A = 60 \div 70$  but the value of about  $E^*/A \simeq 5$  MeV, differs significantly from the ones measured for nuclei in the mass region  $A = 105 \div 135$  suggesting the existence a mass dependence of the limiting excitation energy per nucleon, for the collective motion. Interesting similarities in trend and absolute values can be found when comparing the limiting excitation energy for the collective motion with the energy at which the plateau of the caloric curve sets in, indicating the onset of liquid-gas phase transition. This feature suggests a possible link between GDR disappearance and liquid-gas phase transition which deserves further investigation from both theoretical and experimental points of view. In particular extending the systematics of the GDR to hot nuclei with  $A = 160 \div 180$  could provide further information on the possible link between GDR disappearance and liquid-gas phase transition and therefore shed additional light on the mechanism responsible for the GDR quenching.



- a) Solid symbols represent the spectra after bremsstrahlung subtraction. Open symbols represent the spectra after CASCADE calculations.
- b) Statistical gamma spectra compared to CASCADE calculations shown as red lines.
- c) Linearized Spectra compared to Lorentzian function used in the calculation for each reactions.

# $^{174}\text{W}$ : ORDER-TO-CHAOS TRANSITION

HIGH TEMP

## QUASI-CONTINUUM $\gamma$ - $\gamma$ MATRICES

HIGH TEMP

High-Spin Fusion Evaporation

$^{50}\text{Ti}$  on  $^{128}\text{Te}$  @ 217 MeV,  $I \geq 60\hbar$

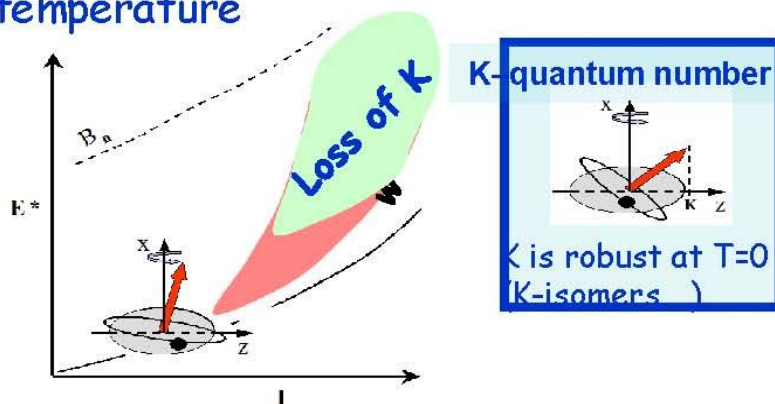
4 Triple Clusters

2 and 3 folds:

$\varepsilon_{2\gamma} = 30\%$ ,  $\varepsilon_{3\gamma} = 10\%$   
( $M_\gamma = 30$ )



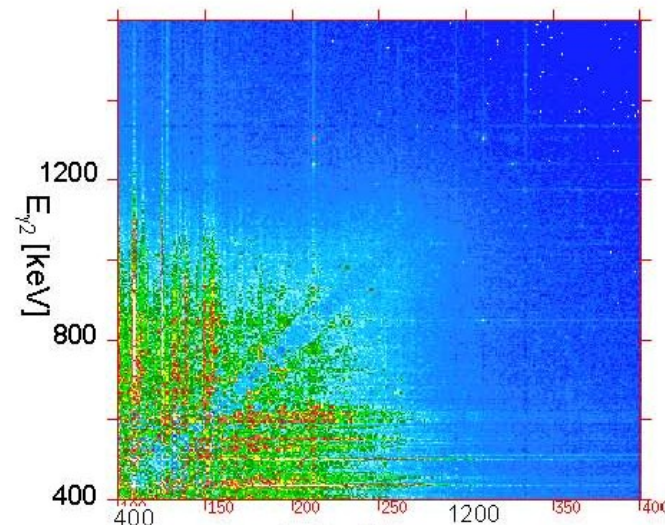
Loss of selection rules on K with temperature



region. The present results suggest that a  $K$ -mixing process due to temperature effects plays an important role already at rather low excitation energy, namely in the onset region of band mixing, here probed by a global analysis of decay properties of the entire body of discrete excited bands. This represents a step forward in the understanding of the basic



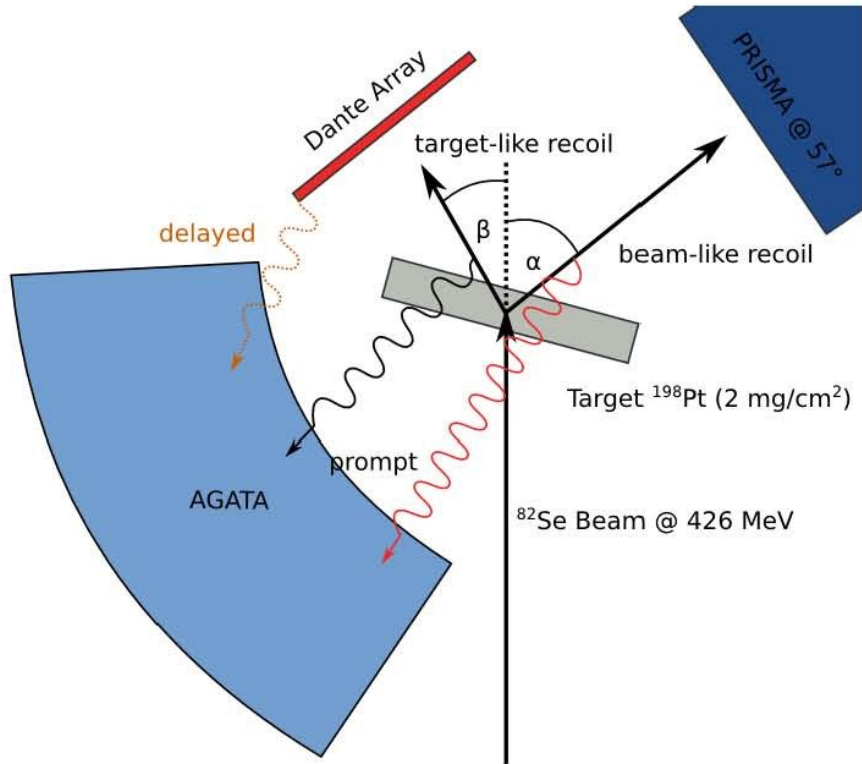
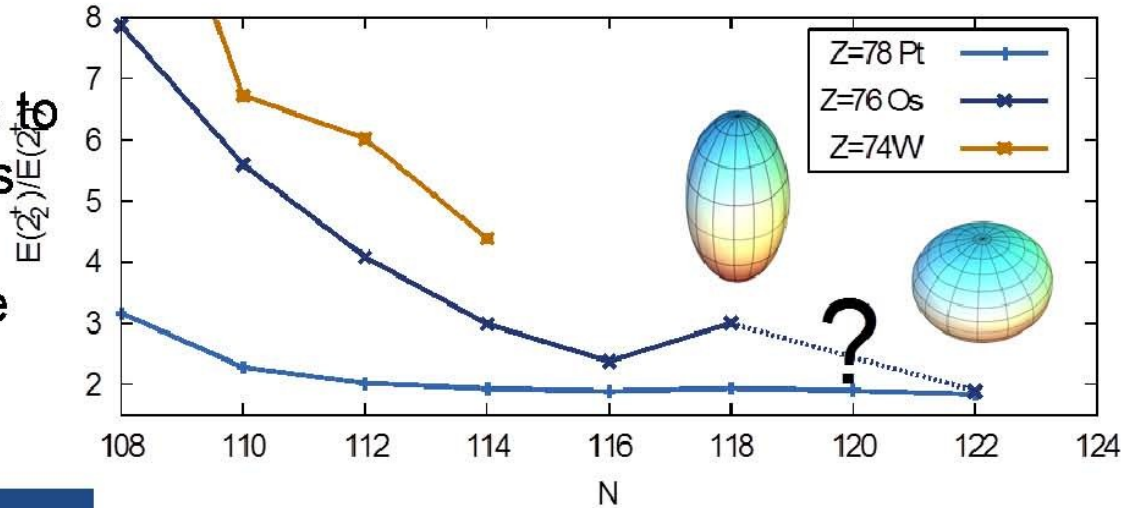
Goal: populate  $^{174}\text{W}$  at the **highest possible spins** ( $\geq 60\hbar$ ), in order to make the **statistical fluctuation analysis of the ridge-valley structures in the  $\gamma$ - $\gamma$  matrices**, to estimate the number of low- $K$  and high- $K$  bands and their correlation



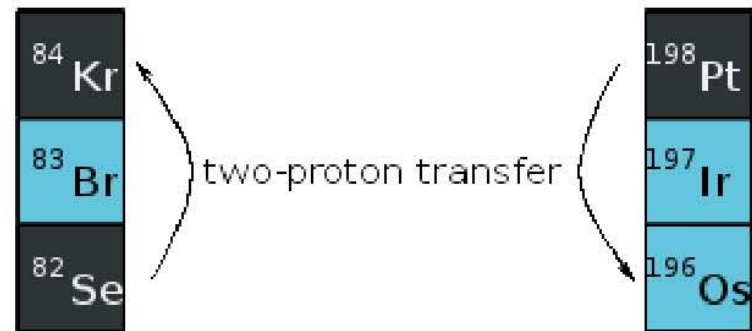
PHYSICAL REVIEW C 88, 034312 (2013)

# SHAPE TRANSITION IN THE OS ISOTOPES

- Shape transition from prolate to oblate deformed nuclei in the Os isotopes
- $^{194}\text{Os}$  suggested to be prolate
- $^{198}\text{Os}$  shows oblate character

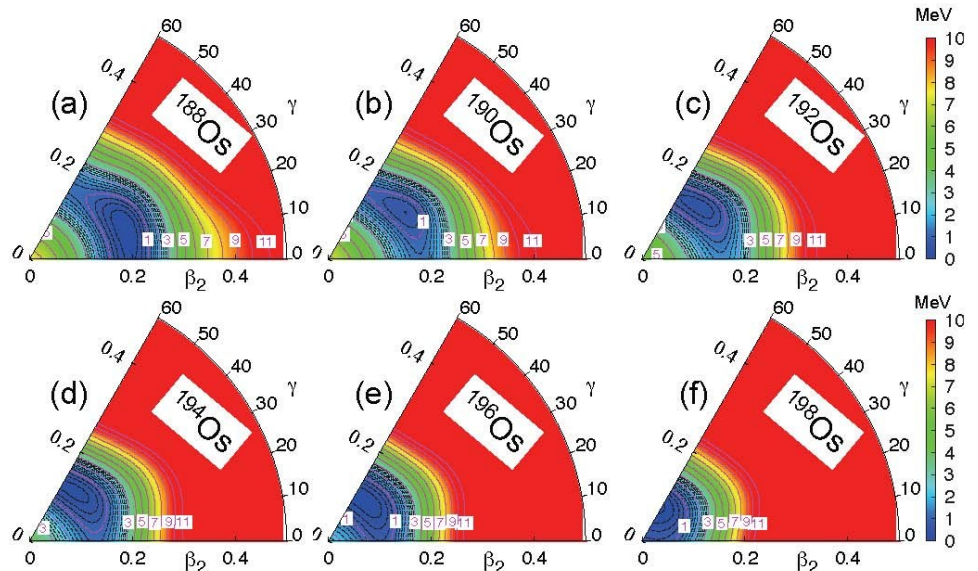
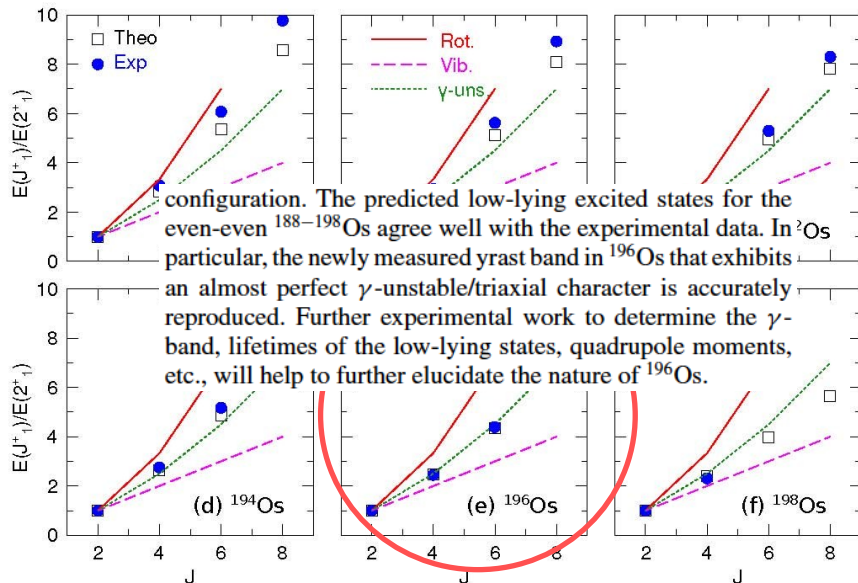
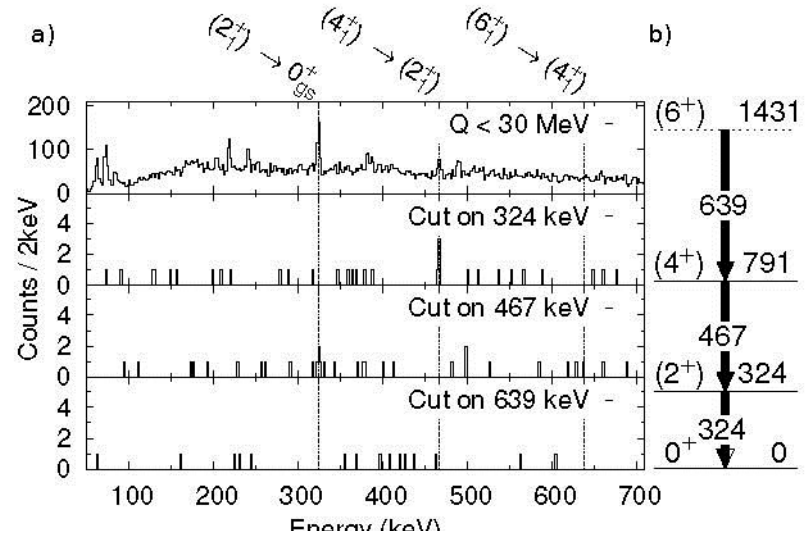
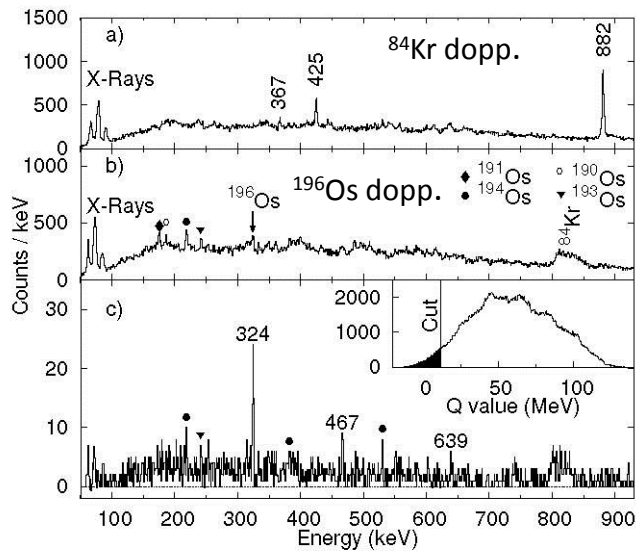


- Binary Partner Method
- $^{82}\text{Se}(^{198}\text{Pt}, ^{196}\text{Os})^{84}\text{Kr}$  @ 426 MeV
- Detect lighter beam-like recoil in PRISMA
- Reconstruct Spectrum for  $^{196}\text{Os}$



# Shape evolution in the n-rich Os isotopes: prompt $\gamma$ -ray spectroscopy of $^{196}\text{Os}$

P.R. John et al. PRC 90 021301 (2014) rapid comm.



Beyond mean field with generator coordinate method  
 Mixing particle num. and ang. Mom. projected states

# Superdeformation in $A \sim 40$ nuclei

E. Ideguchi (RCNP, Osaka Univ.) – January 2013

Search for superdeformed bands in  $^{35,36}\text{S}$ ,  $^{40}\text{Ar}$  via  $^{18}\text{O} + ^{26}\text{Mg} \rightarrow ^{44}\text{Ca}^*$

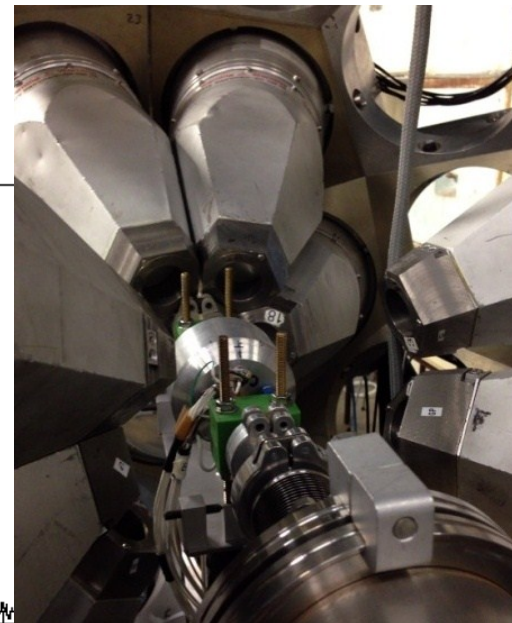
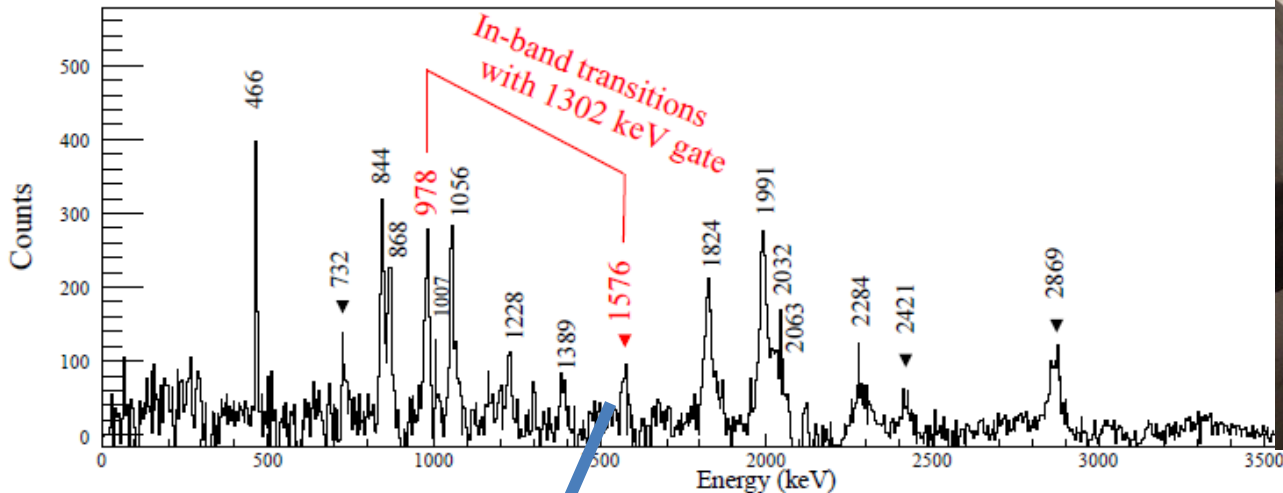


Fig. 1.  $\gamma$ -ray energy spectrum gated 1302-keV transition. The 1576-, 1302- and 978-keV transitions belong to the same band transition. The peaks labeled with the triangles are new transitions of  $^{35}\text{S}$ .

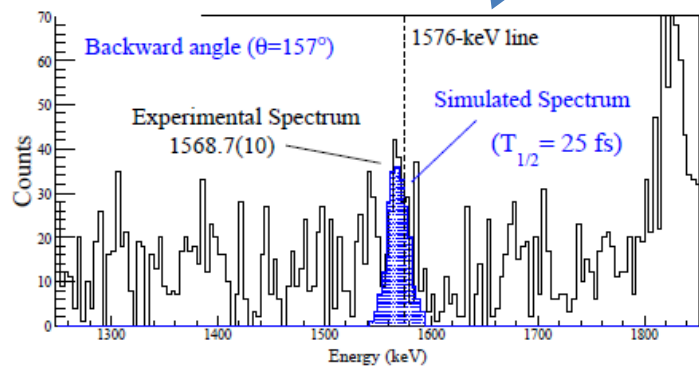


Fig. 2. Comparison between experimental and simulated spectra for the residual Doppler shifted 1576-keV peak in the forward and backward angles of the germanium detectors.

Investigations of the orbitals responsible for superdeformation in the mass region,  $f_{7/2}$ , nearby are important to infer the existence of superdeformed states in  $^{32}\text{S}$ .

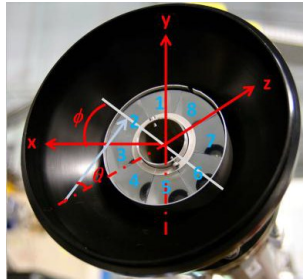
The de-excitation of the superdeformed band was observed from  $19/2^-$  to  $7/2^-$ . The superdeformed band structure was highlighted by the measurement of half-life and relative intensities of the intra-band transition. The  $f_{7/2}$  negative parity intruder orbital seems to be responsible for the negative

# Time Dependent Recoil In Vacuum on H-like ions:

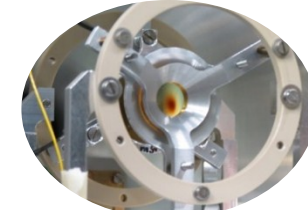
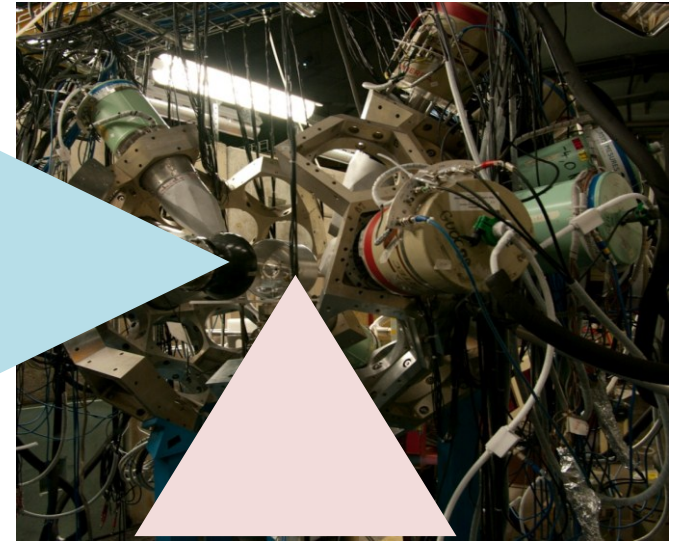
## $^{24}\text{Mg}$ - revisited

G. Georgiev (CSNSM), A.E. Stuchbery (ANU), Dec. 2012

- *Experiment:* **High accuracy** ( $< 2\%$ ) **model independent** ( $B$  from *first principles*) **g-factor** value for short-lived (ps) excited states
- *Theory:* **g-factors** of the  $2^+$  states in  $N=Z$  nuclei should be **slightly higher than 0.5**

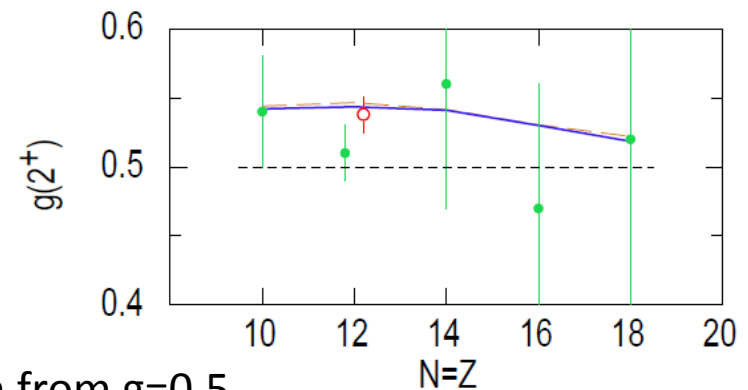
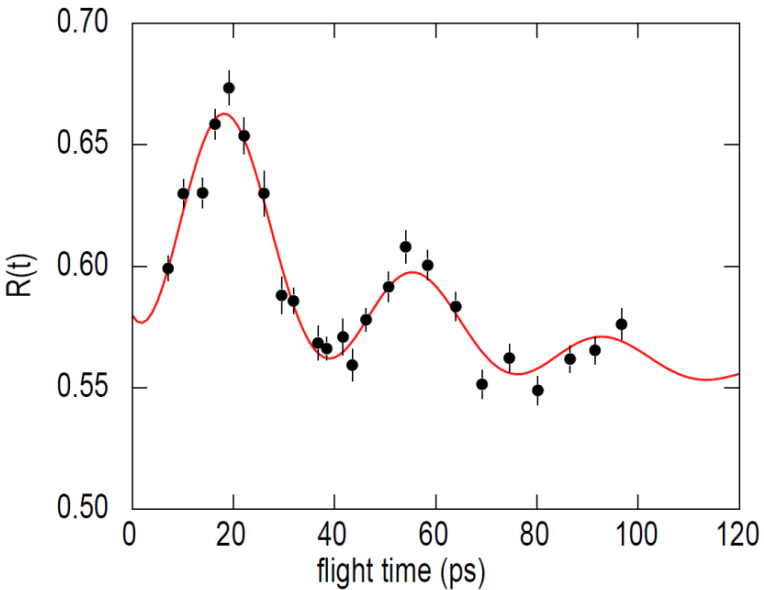


8-fold segmented annular detector



OUPS  
(Orsay Universal  
Plunger System)

$^{24}\text{Mg}+^{93}\text{Nb}$  coulex



A. Kusoglu, A. Stuchbery, G. Georgiev *et al.*

*Our result:* **first experimental evidence** of deviation from  $g=0.5$   
→ stringent test of the nuclear theories

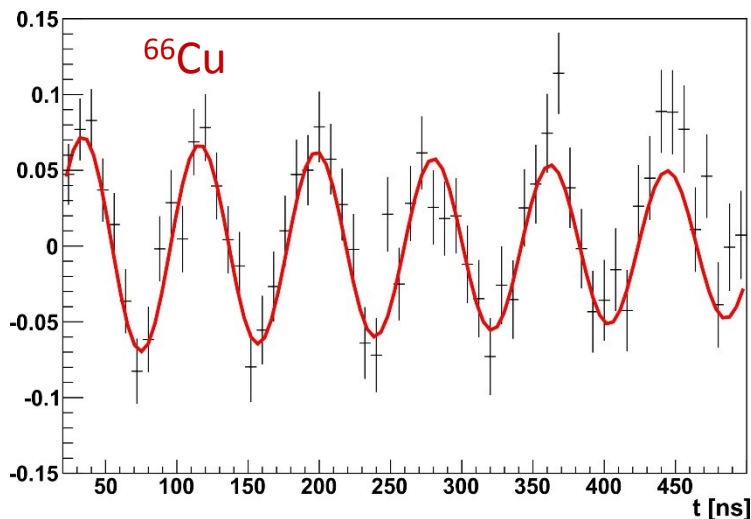
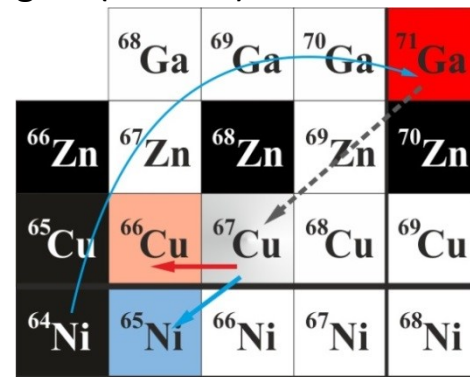


# Nuclear spin orientation in incomplete fusion reactions

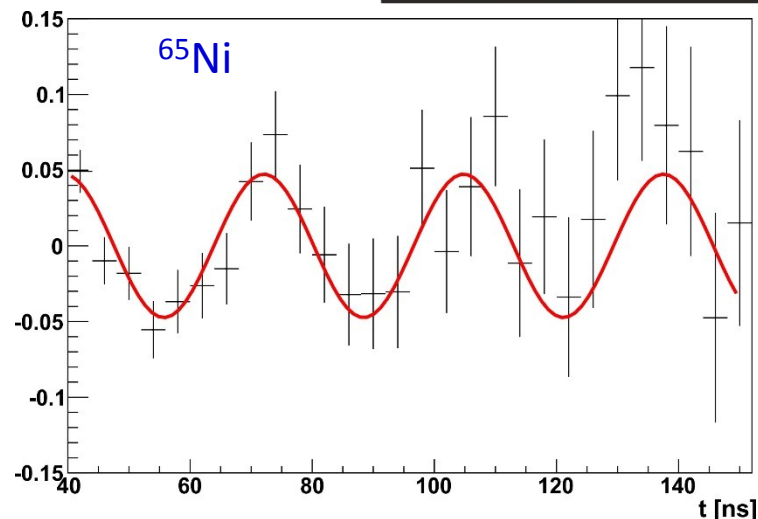
G. Georgiev (CSNSM) Dec. 2013

**Nuclear spin orientation** – a must for nuclear moments studies

- Fusion-evaporation reactions – 25 % - 75 % alignment
- Projectile-fragmentation - 8 % - 13 %
- Direct reactions (single-nucleon transfer) ~ 13 %
- **Incomplete fusion** (multi-nucleon transfer?) – ???



Amplitude = 8 (1) %  
**Spin alignment = 23 (3) %**



Amplitude = 4.8 (8) %  
**Spin alignment = 12.5 (20) %**

Results:

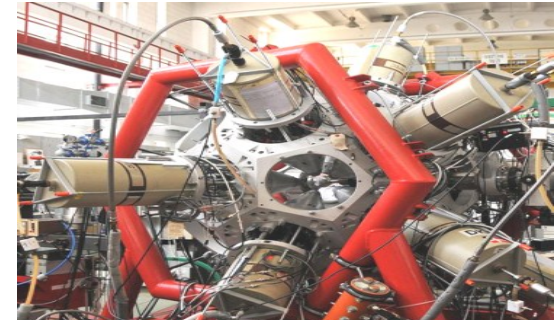
- considerable spin alignment in  $^7\text{Li}$  induced reactions;
- dependence on the number of transferred nucleons?

$^7\text{Li}+^{64}\text{Ni}$   
 Triton 1n ,  
 triton1pn

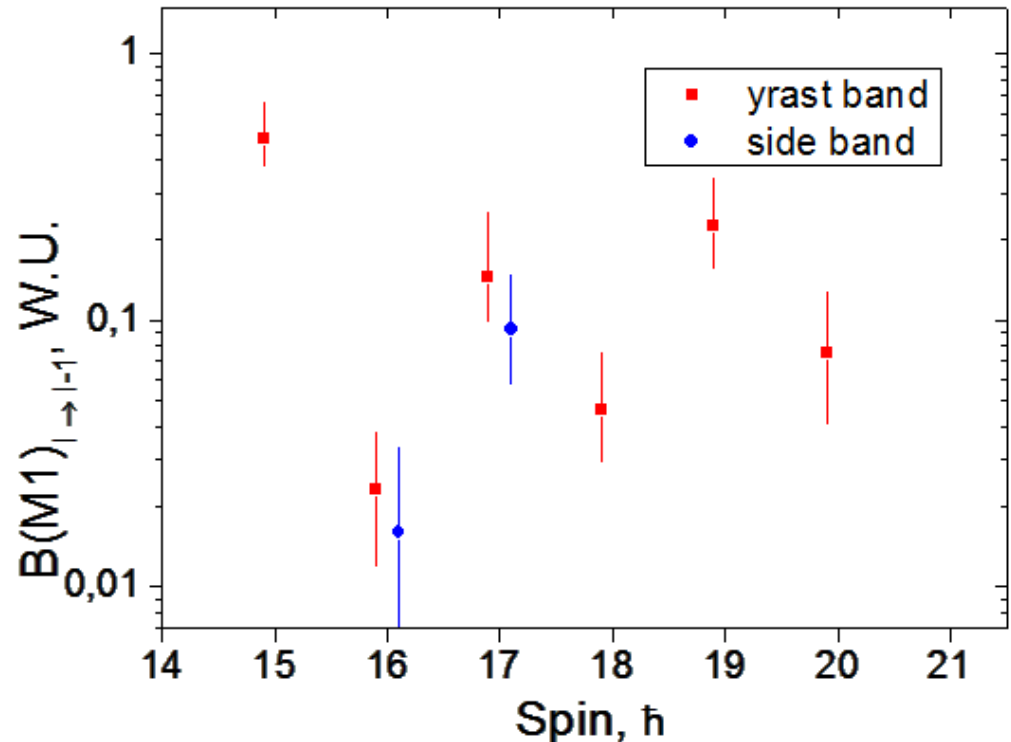
# Spontaneous chiral symmetry breaking in $^{124}\text{Cs}$

The central European Array for Gamma Levels Evaluation

- Experiment - EAGLE [1] array.
- DSA method measurement leading to  $B(M1)$  and  $B(E2)$  determination.
- Spontaneous chiral symmetry breaking [2] is proven if one can see two rotational partner bands (chiral partner bands) with similar reduced transition probabilities, ( $B(M1)$  and  $B(E2)$ )).



Preliminary results for  $^{124}\text{Cs}$   
-  $B(M1)$  in partner bands.

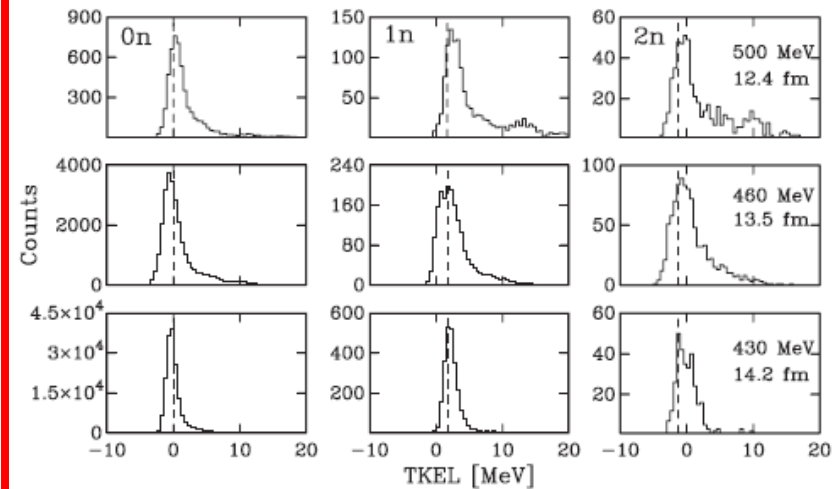
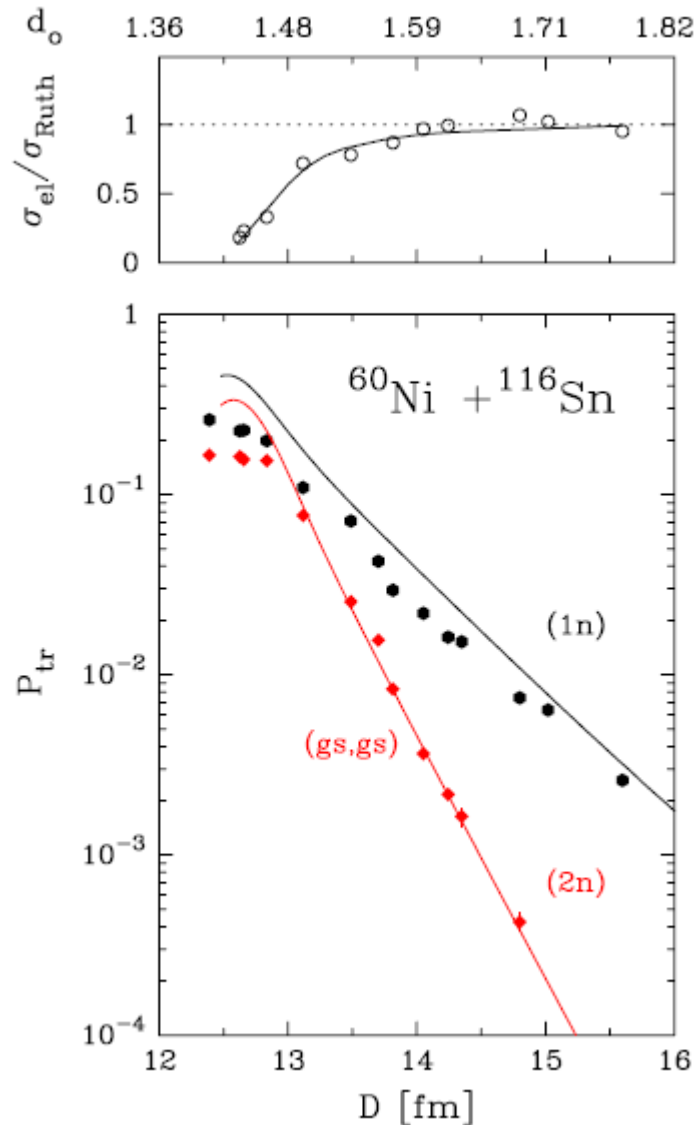


[1] J. Mierzejewski et al., NIM A 659, 84 (2011).

[2] E. Grodner et al., Eur. Phys. J A27, 325 (2006).

# Neutron pair transfer in $^{60}\text{Ni}+^{116}\text{Sn}$ far below the Coulomb barrier

Transfer strength very close to the g.s. to g.s. transitions



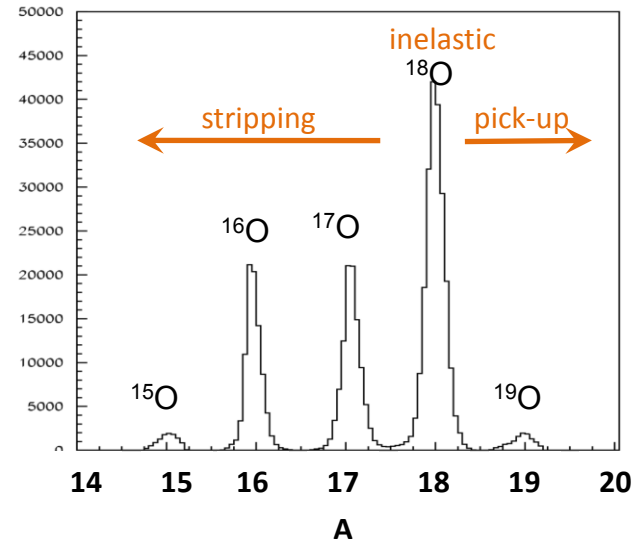
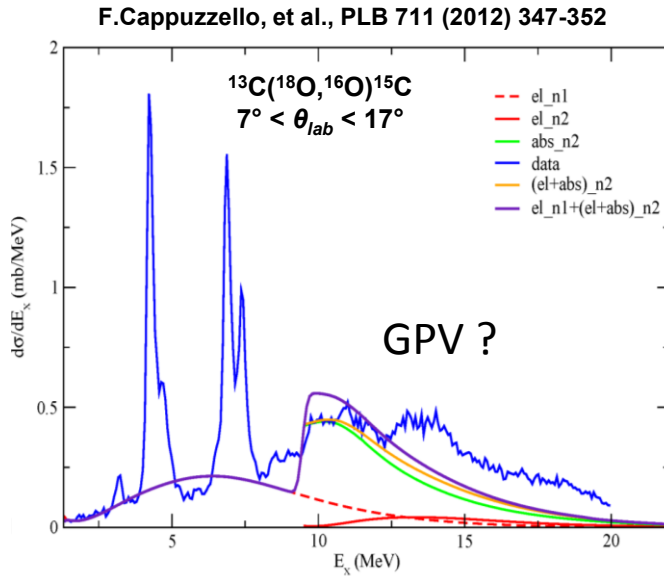
The experimental transfer probabilities are well reproduced, for the first time with heavy ion reactions, in absolute values and in slope by microscopic calculations which incorporate nucleon-nucleon pairing correlations



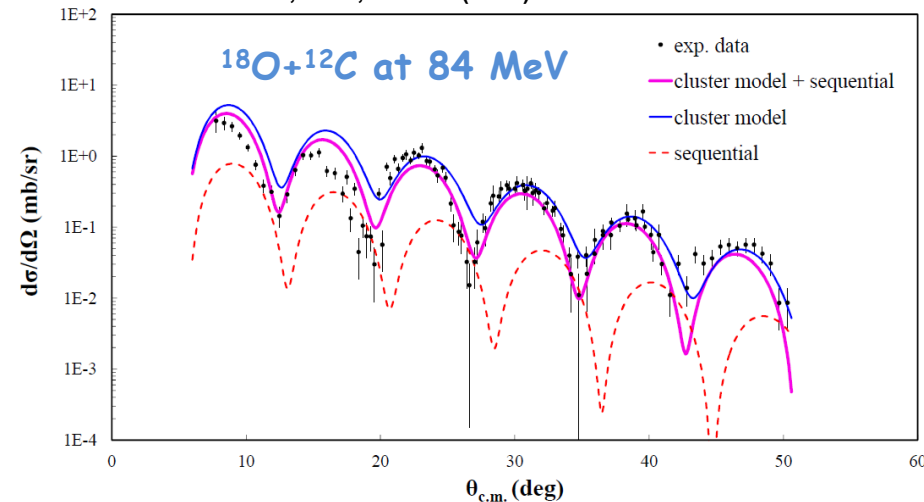
# Pairing correlations with MAGNEX

$^{18}\text{O}+^{13}\text{C}$  at 84 MeV

$7^\circ < \vartheta_{lab} < 13^\circ$



M.Cavallaro, et al., PRC 88 (2013) 054601

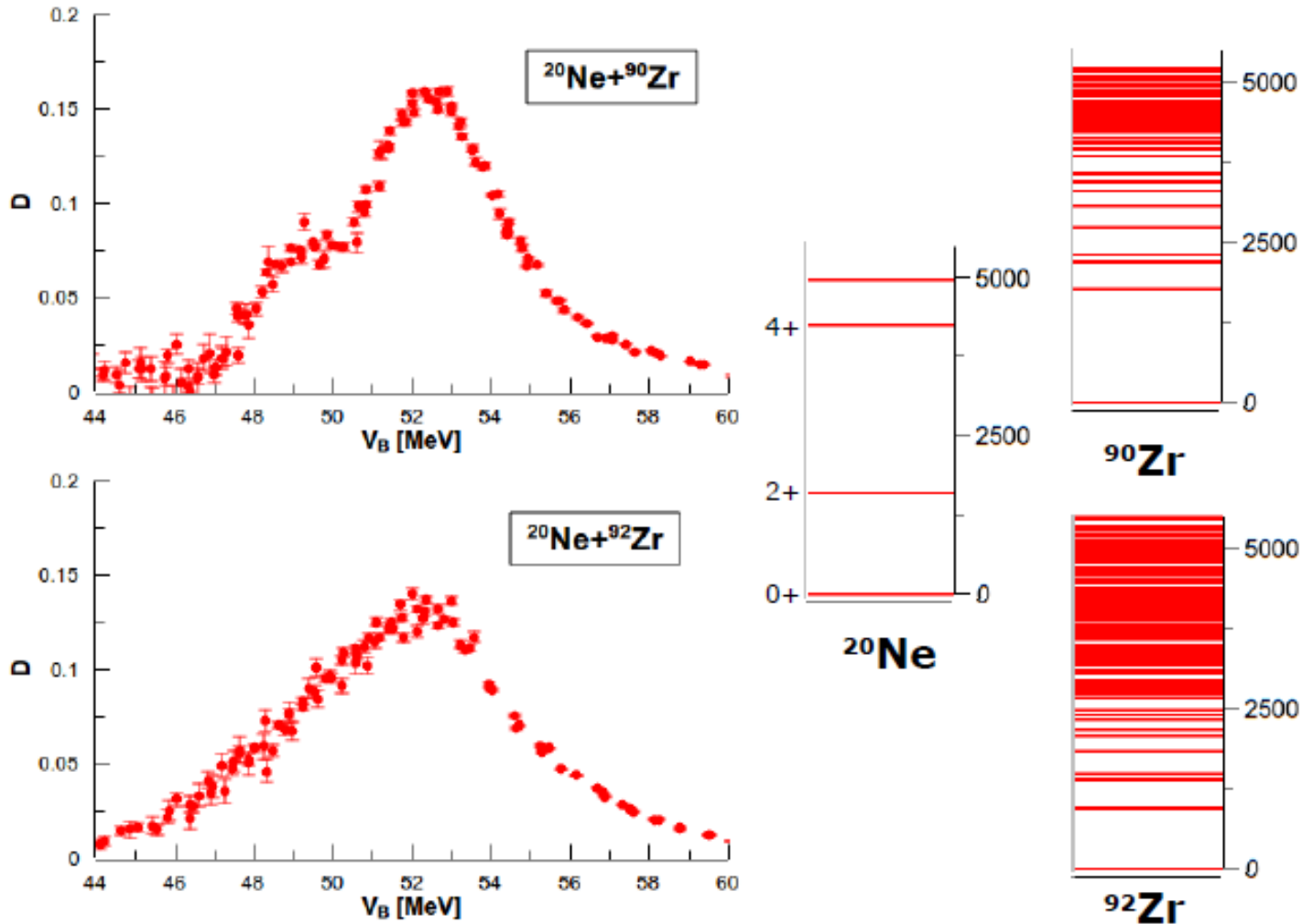


- ✓ Major physics output, observation of GPV (?) **correlated two-neutron transfer**, determination of **pair spectroscopic amplitude**

D.Carbone Thesis (2013)  
 and manuscript submitted

# Barrier distributions for fusion

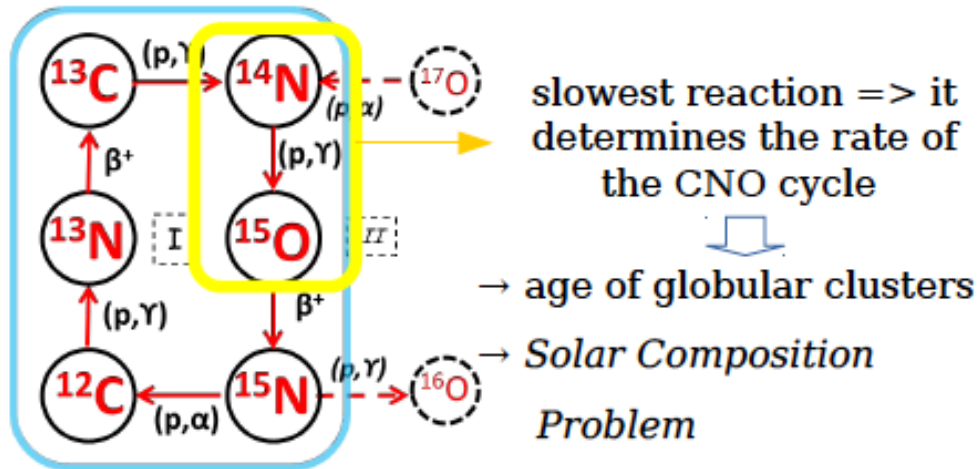
ŚRODOWISKOWE LABORATORIUM  
CIĘŻKICH JONÓW



Recent papers: E. Piasecki et al. PRC 85 (2012) 054604 and 054608

NAP

## Stellar burning rates and $^{14}\text{N}(p,\gamma)^{15}\text{O}$ reaction

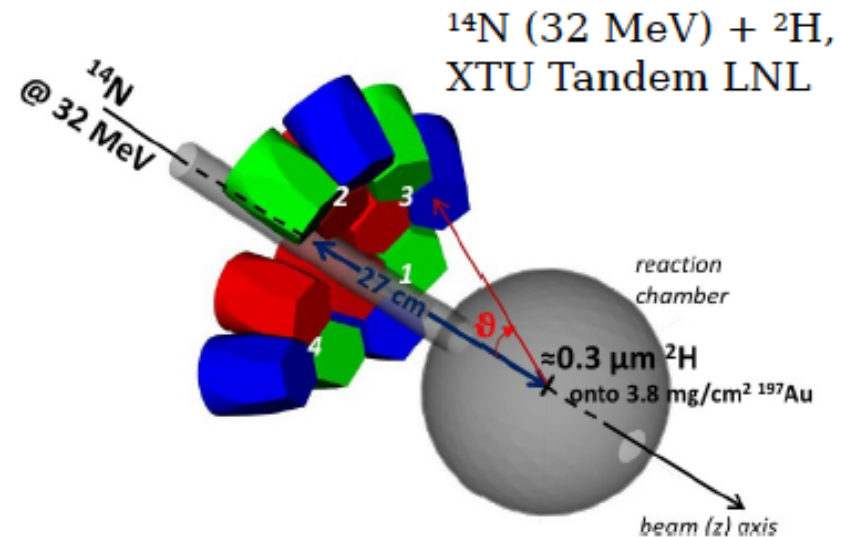


The sub-threshold resonance corresponding to the first excited  $3/2^\pm$  state in  $^{15}\text{O}$  is predicted to play a dominant role when extrapolating the cross-section to the Gamow peak region

**width of the resonance  $\Leftrightarrow$  lifetime of the nuclear state**

**First application of the high gamma energy resolution and position sensitivity of AGATA to investigate  $\approx$ fs nuclear level lifetimes**

## Lifetime measurement of the 6.79 MeV state in $^{15}\text{O}$ with the AGATA Demonstrator

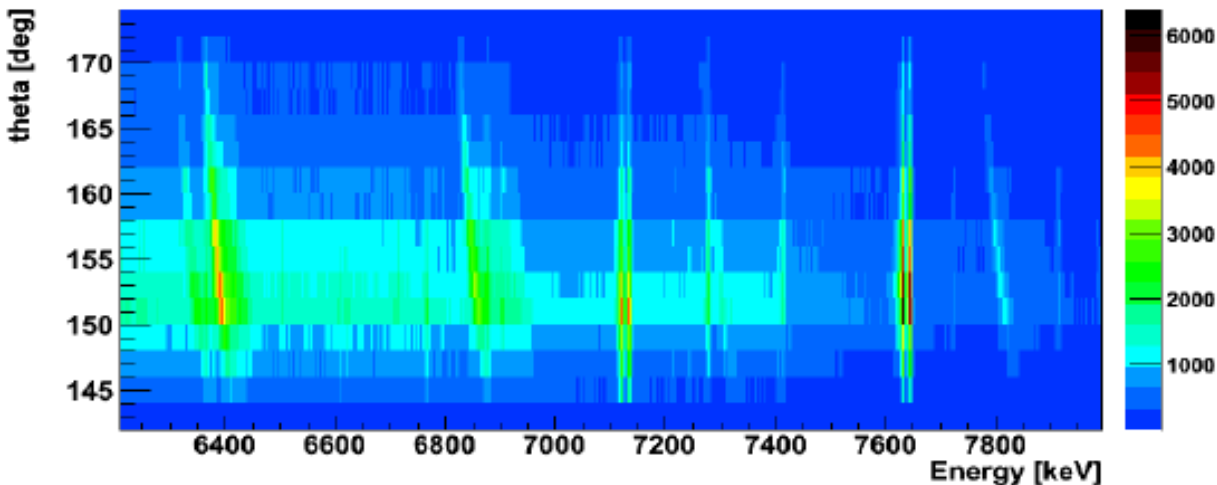


4 asymmetric triple-clusters  
12 36-fold segmented HPGe

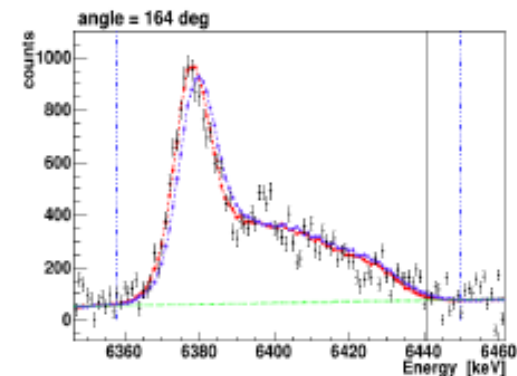
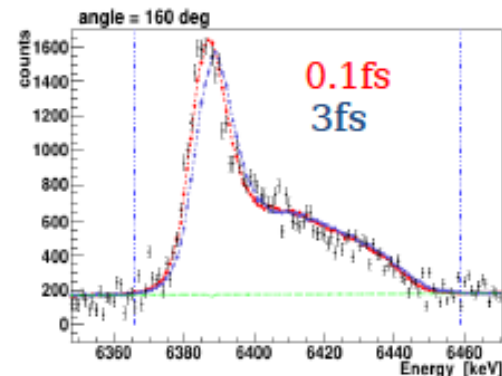


first interaction point and  $\gamma$  energy event-by-event:  
Lineshape analysis with a few degrees resolution

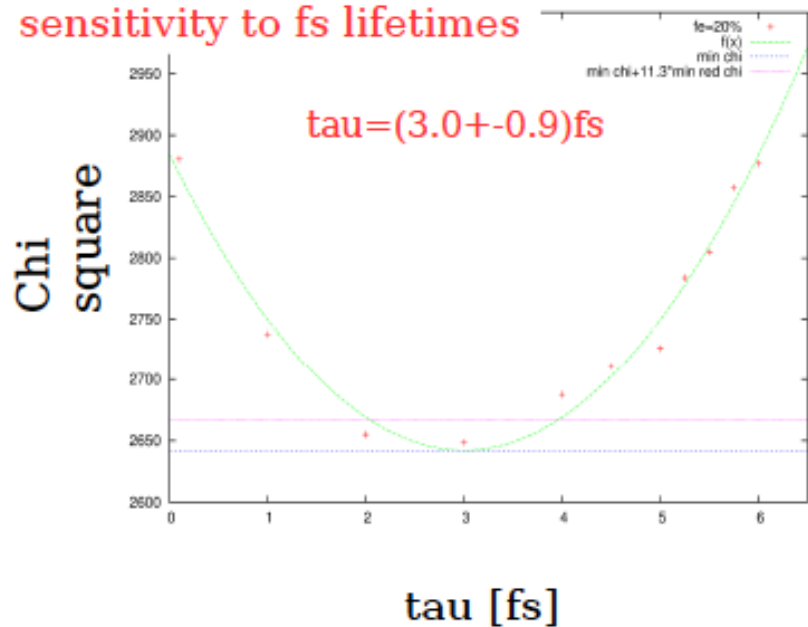
## Energy vs theta first interaction point



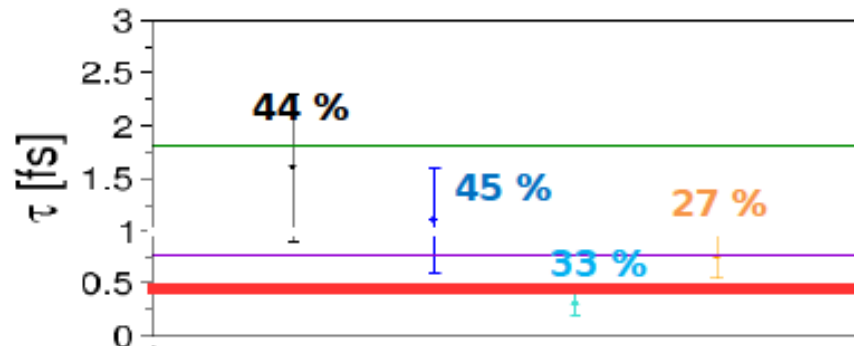
## Lineshape analysis for the 6.79 MeV state in $^{15}\text{O}$



## 8.31 MeV level in $^{15}\text{N}$ : sensitivity to fs lifetimes

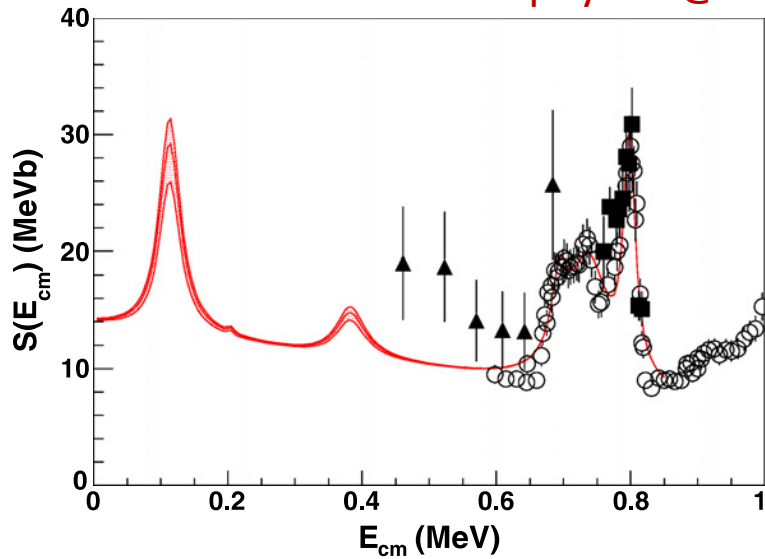


## New upper limit on the lifetime of the 6.79 MeV state in $^{15}\text{O}$





# Nuclear astrophysics @ LNS – Trojan Horse Method Applications



THM is an indirect method that allow to extract nuclear information of a two-body reaction, even at astrophysical energies, by means of the quasi-free contribution in an appropriate three-body reaction.



$^{19}\text{F}(p,\alpha)^{16}\text{O}$  (two-body reaction) studied at LNS via

$^{19}\text{F}(d,\alpha n)^{16}\text{O}$  (three-body reaction)

At 50 MeV @Tandem

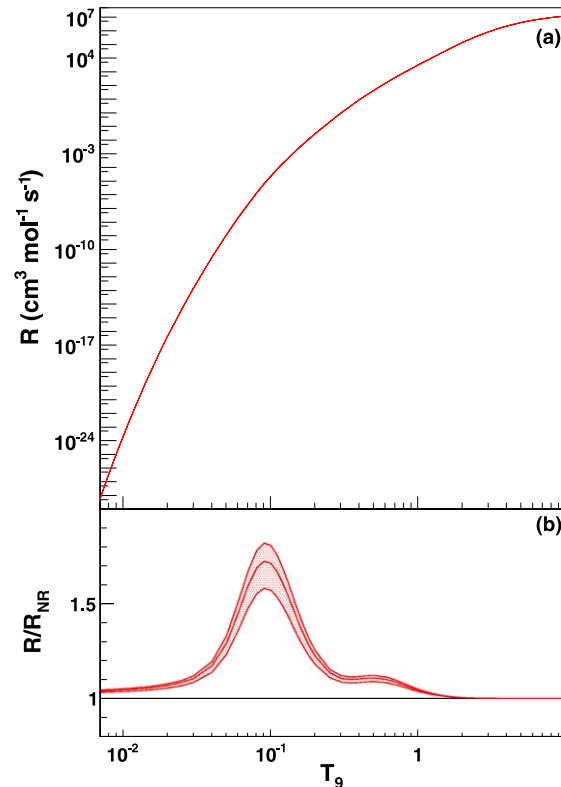
Red line Rmatrix based on THM data  
Points, direct measurements

First time in Gamow window (<500 keV)

Reaction rate is calculated in the AGB star temperature window for the first time.

The ratio to the NACRE evaluation is reported in panel b

THE ASTROPHYSICAL JOURNAL LETTERS, 739:L54 (6pp), 2011 October 1  
© 2011. The American Astronomical Society. All rights reserved. Printed in the U.S.A.



# Search for new resonant states in $^{10}\text{C}$ and $^{11}\text{C}$ and their impact on the cosmological lithium problem

F. Hammache, N. de Sereville, I. Stefan

Primordial nucleosynthesis (BBN) is one of the three evidences for the Big-Bang model

When  $T < 10^9$  K  $\rightarrow$  BBN starts

- Production of  $\text{D}$ ,  $^3\text{He}$ ,  $^4\text{He}$ ,  $^7\text{Li}$
- Abundances depend on baryonic density

$\text{D}$ ,  $^3\text{He}$ ,  $^4\text{He}$ , observations agree with predictions (BBN + CMB)

Metal poor halo dwarf stars



$${}^7\text{Li problem: } ({}^7\text{Li}/\text{H})_{\text{BBN}} / ({}^7\text{Li}/\text{H})_{\text{obs}} = 4$$

## Possible explanations:

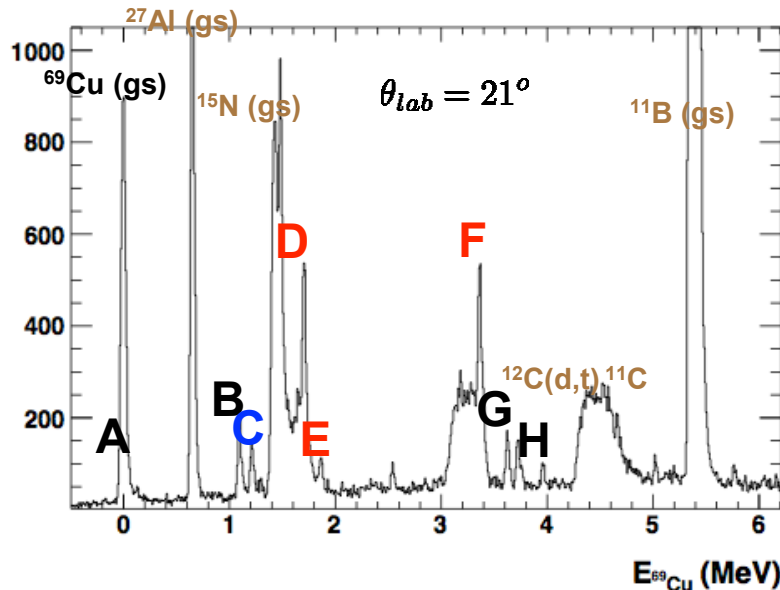
- Physics beyond standard model: super-symmetry, constant variation, ....
- Observations: can  $^7\text{Li}$  be uniformly destroyed in the Spite plateau region?
- Nuclear physics:  $^7\text{Li}$  produced by  $^7\text{Be}$  EC &  $^3\text{He}(^4\text{He}, \gamma)^7\text{Be}$  known better than 15%

## Last proposed solution studied with SPLITPOLE @ IPN Orsay

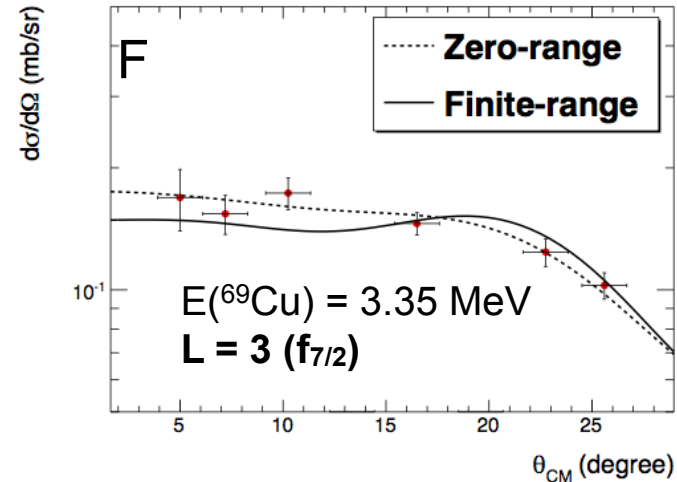
Finally, our two results concerning  $^{10}\text{C}$  and  $^{11}\text{C}$  compound nuclei put an end to the various discussions concerning the missing resonant states in these nuclei, which were thought to partially or totally solve the  $^7\text{Li}$  problem [19–21] and exclude  $^7\text{Be} + ^3\text{He}$  and  $^7\text{Be} + ^4\text{He}$  reaction channels as responsible for the observed  $^7\text{Li}$  deficit.

Direct kinematics  $^{70}\text{Zn}(d, ^3\text{He})^{69}\text{Cu}$  with 27 MeV deuteron beam and SPLITPOLE spectrometer

Part of the program: Systematic of the evolution for  $f_{7/2}$  proton-hole strength from stability to  $^{78}\text{Ni}$  ?



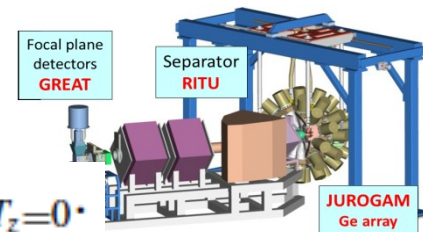
### Angular distribution for the f state



Excitation energy of  $^{69}\text{Cu}$  measured with splitpole.  
Letters correspond to states in  $^{69}\text{Cu}$

$E$ (MeV)	$L (J^\pi)$	$C^2S$ (ZR)	$C^2S$ (FR)
0	1 ( $3/2^-$ )	1.40(15)	1.50(17)
1.10	-	-	-
1.23	3 ( $5/2^-$ )	0.80(11)	0.70(10)
1.71	3 ( $7/2^-$ )	2.00(11)	2.50(14)
1.87	3 ( $7/2^-$ )	0.40(10)	0.50(10)
3.35	3 ( $7/2^-$ )	1.60(10)	2.40(15)
3.70	2 ( $3/2^+$ )	1.90(25)	1.50(20)
3.94	0 ( $1/2^+$ )	0.70(06)	0.70(10)

New part of the  $f_{7/2}$  strength:  $\sum f_{7/2} = 5.40$  or 67%

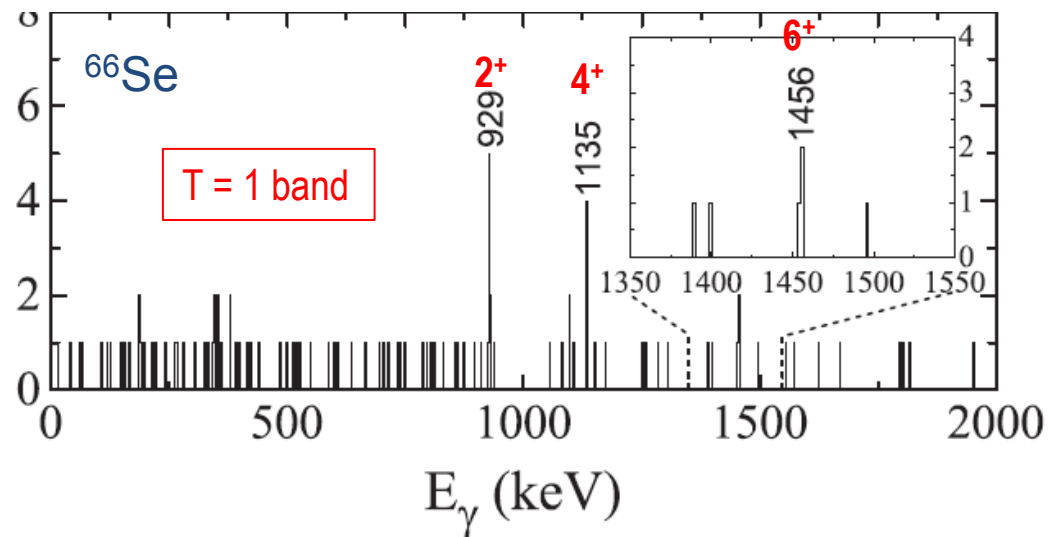


$$TED_{J,T} = E_{J,T,T_z=-1}^* + E_{J,T,T_z=+1}^* - 2E_{J,T,T_z=0}^*$$

**Spectroscopy of proton-rich  $^{66}\text{Se}$  up to  $J^\pi = 6^+$ :  
Isospin-breaking effect in the  $A = 66$  isobaric triplet**

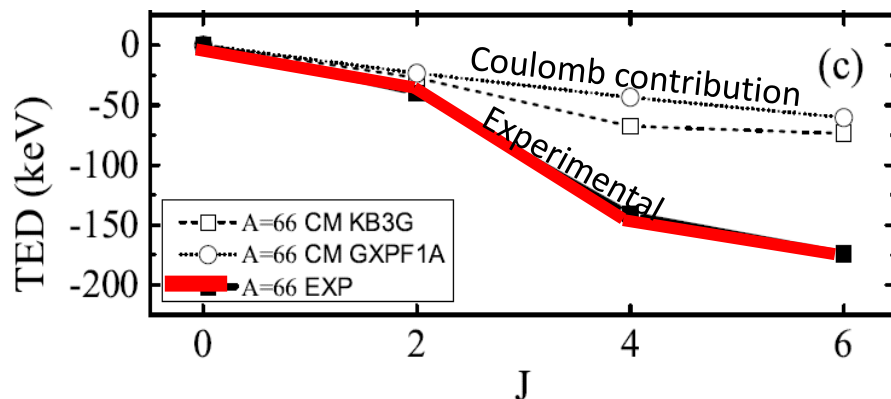
## Recoil-beta tagging study:

- $^{40}\text{Ca}(^{28}\text{Si}, 2n) ^{66}\text{Se} \sim 200\text{nb}$
- UoY **Tube** Charged-particle veto
- $^{66}\text{As}$  isomer veto-tagging



TED=Triple Energy Differences  
for the  $A = 66$   $T=1$  triplet

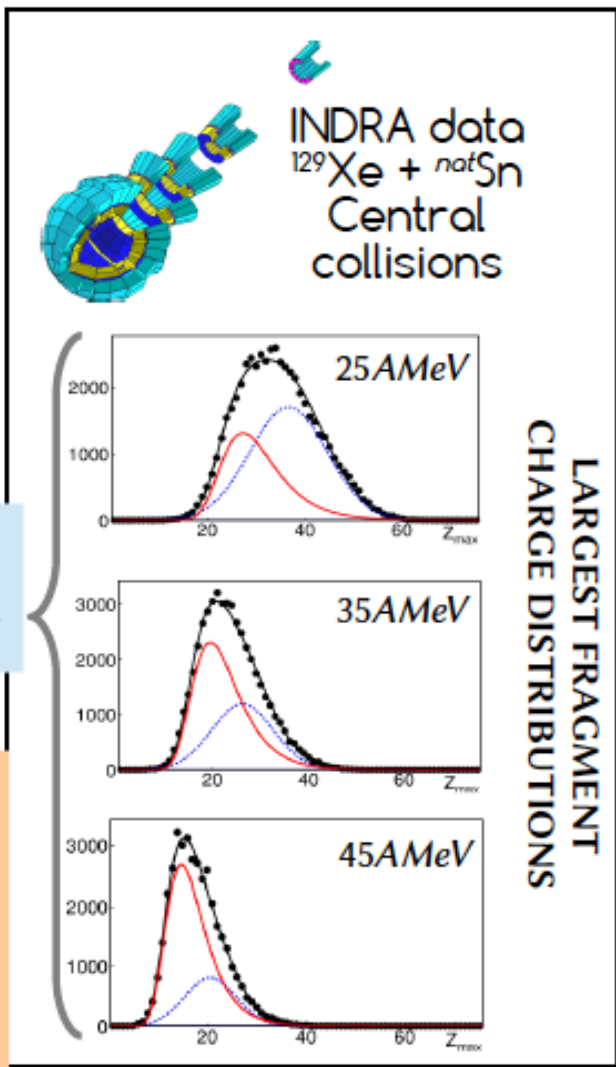
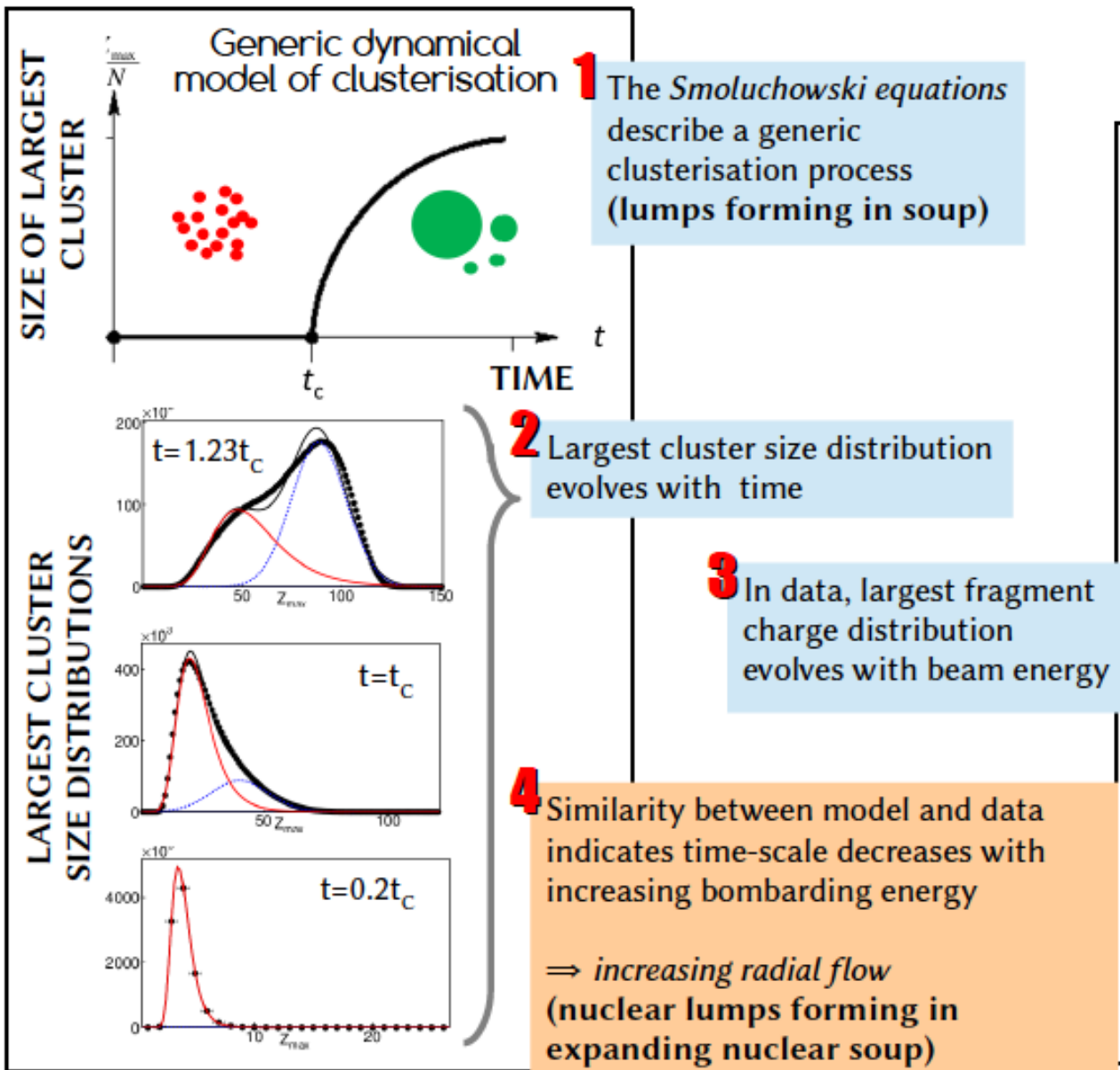
*Isospin non-conserving  
contribution is needed !*



Timescale of the multifragmentation is directly reflected in the shape of the largest fragment charge/mass distribution

INDRA collaboration  
 +M. Ploszajczak (GANIL)  
 +R. Botet (LPS Orsay)

D. Gruyer et al.,  
 Phys. Rev. Lett. 110, 172701 (2013)



## CHIMERA@LNS



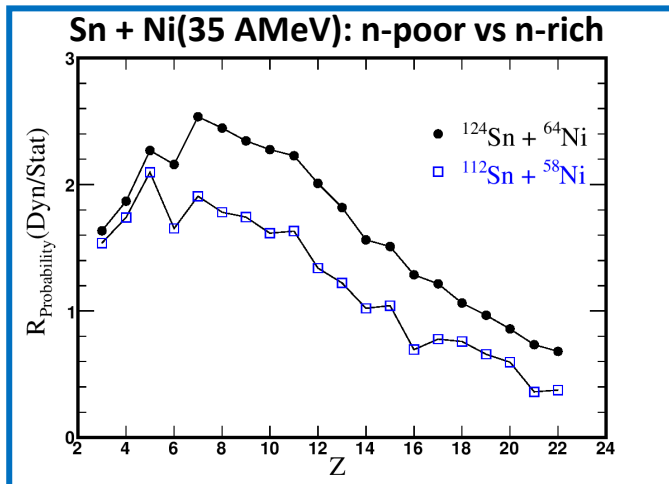
A.Pagano et al., NPA734 (2004)

- ❑ Reaction Dynamics at Fermi energy (\*)
- ❑ EOS - density dependence of the symmetry term (\*\*)
- ❑ Reactions and Structure with Radioactive Fragmentation Beam (\*\*\*)
- ❑ Correlation and interferometry : FARCOS (\*\*\*\*)  
DSSD(300+1500+Csi)

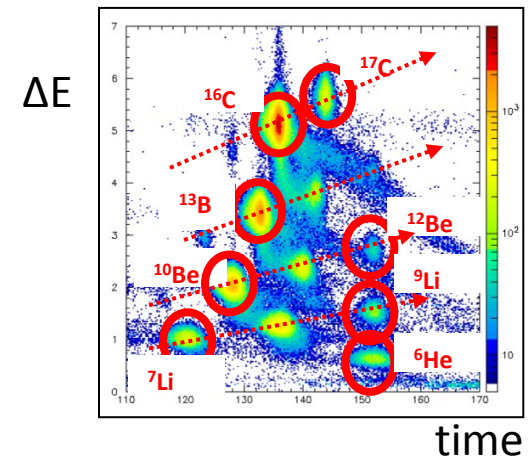
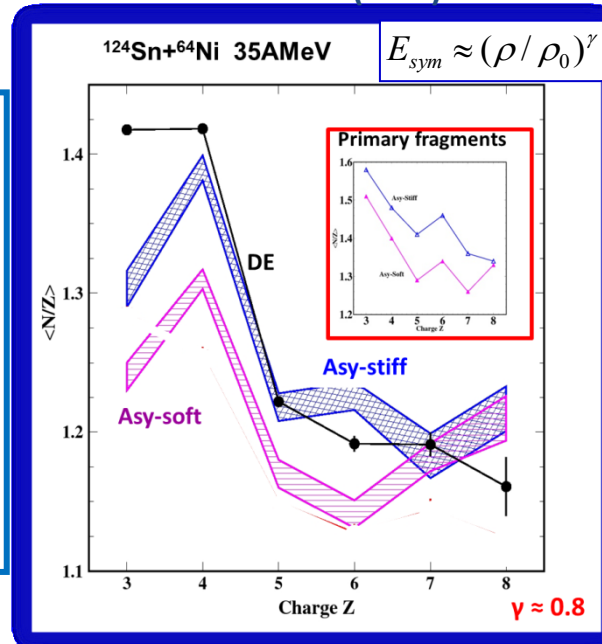
(\*\*\*) In-Flight RIB production

IT NEEDS HIGH INTENSITY BEAMS

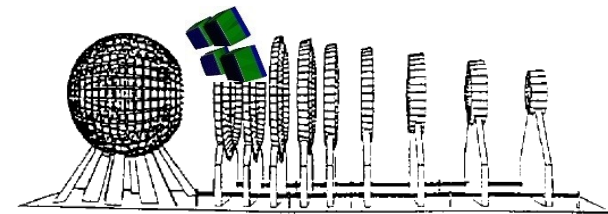
(\*) Dyn/Stat Fission:  
Size or Isospin effects?

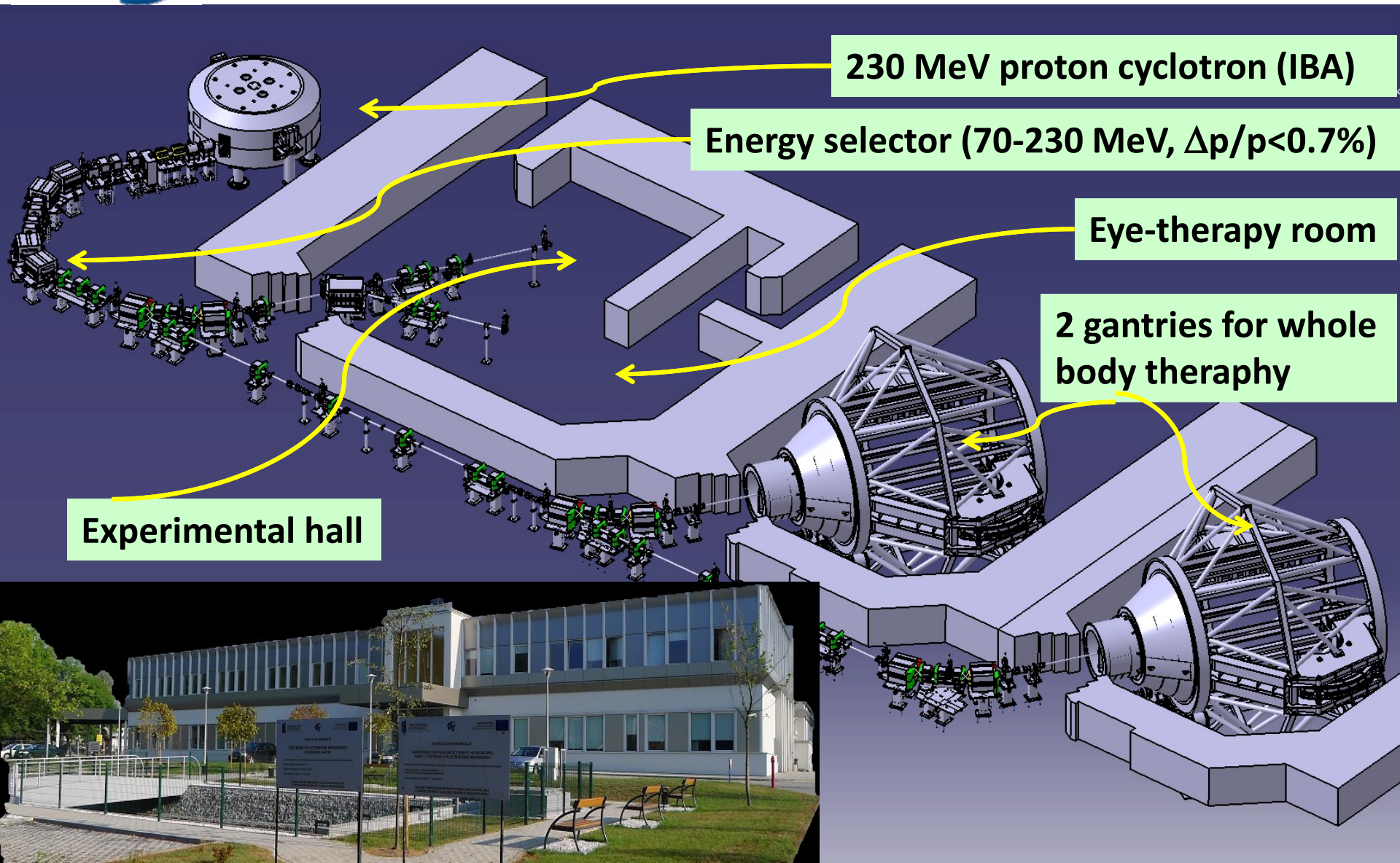


(\*\*) Comparison of IMF data with Stochastic Mean Field (SMF) + GEMINI



(\*\*\*\*) CHIMERA + FARCOS correlator





## B) Study of the dynamics of few-body systems

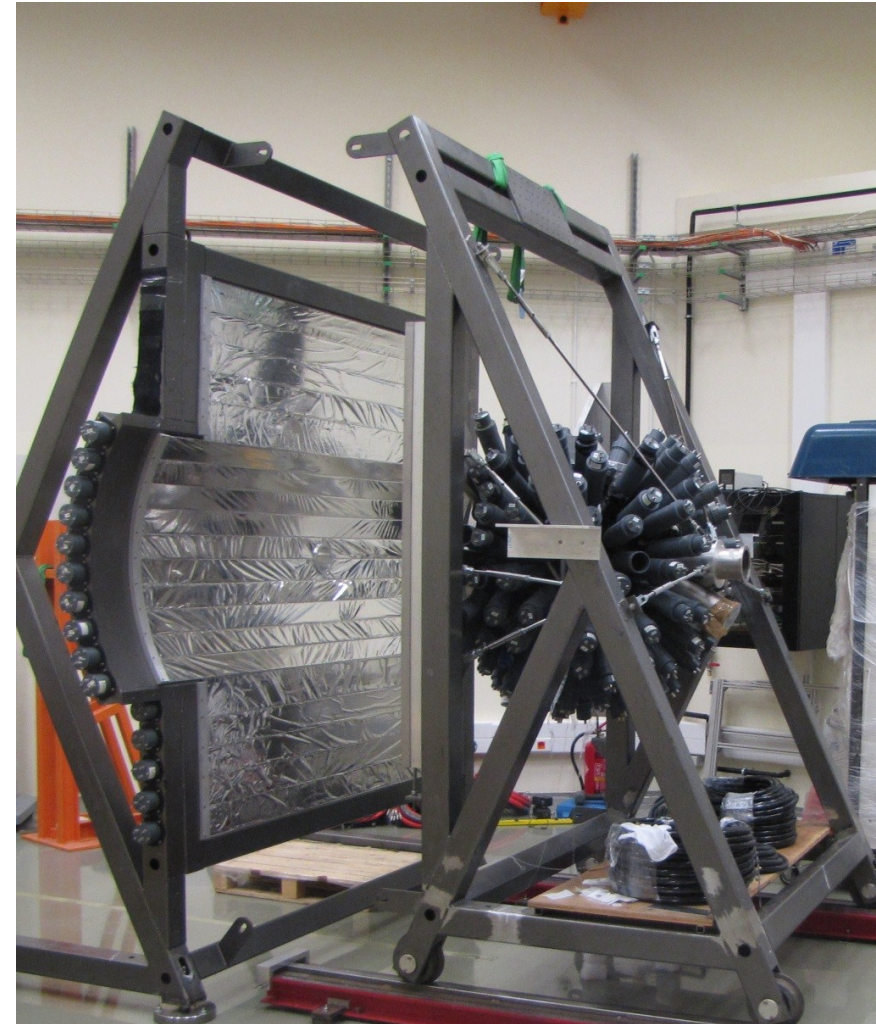
1. Detector **BINA** (moved from KVI Groningen) for light nuclei reactions studies

Wall:

- MWPC (3 planes)
- $\Delta E$  (24 x 2 mm)
- E (20 x 120 mm)

Ball:

- Phoswich (149 x 90/30 mm)



CCB Krakow and HIL Warsaw are in the ENSAR2 H2020 project as TNA facility



To Boldly Go Where No Man  
Has Gone Before...



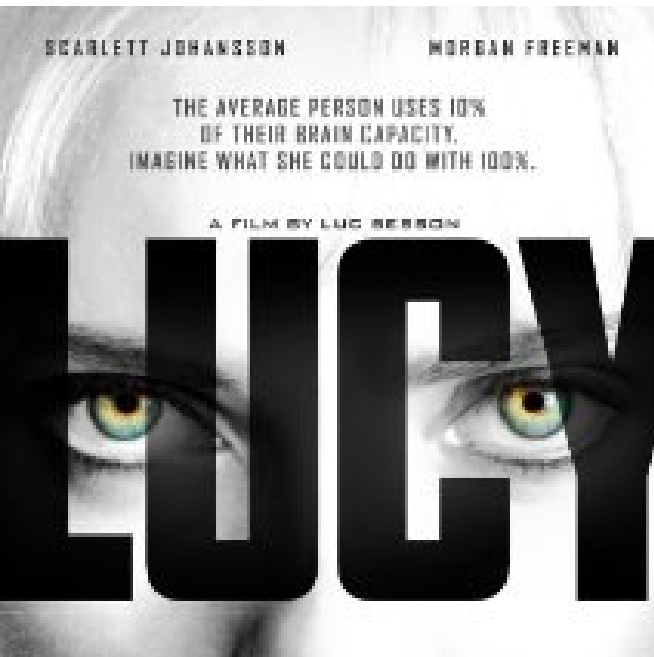
## *ECOS: a Path to ...*

What can we do differently that we cannot do today?

*What are the physics questions that we specifically want to address for which we need very intense stable beams ?*

*What are the things we need to think and develop (other than the machine)*

(Other speakers are going to answer this)



*Evolution to revolution*

